MMI-2017-16697 revised manuscript

The TPR domain of BepA is required for productive interaction with substrate proteins and the β-barrel assembly machinery (BAM) complex

Running title: Structure and function of BepA TPR domain

Yasushi Daimon[1], Chigusa Iwama (Masui)[1], Yoshiki Tanaka[2], Takuya Shiota[3], Takehiro Suzuki[4], Ryoji Miyazaki[1], Hiroto Sakurada[2], Trevor Lithgow[3], Naoshi Dohmae[4], Hiroyuki Mori[1], Tomoya Tsukazaki[2, *], Shin-ichiro Narita[5, *], Yoshinori Akiyama[1, *]

[1]Institute for Frontier Life and Medical Sciences, Kyoto University, Kyoto 606-8507, Japan; [2]Graduate School of Biological Sciences, Nara Institute of Science and Technology, Nara 630-0192, Japan; [3]Biomedicine Discovery Institute and Department of Microbiology, Monash University, Victoria 3800, Australia; [4]Biomolecular Characterization Unit, Center for Sustainable Resource Science, RIKEN, Saitama 351-0198, Japan; [5]Faculty of Nutritional Sciences, University of Morioka, Iwate 020-0694, Japan

*For correspondence:
Yoshinori Akiyama, Institute for Frontier Life and Medical Sciences, Kyoto University, Kyoto 606-8507, Japan. Phone: +81-75-751-4040, E-mail: yakiyama@infront.kyoto-u.ac.jp

For Peer Review

Shin-ichiro Narita, Faculty of Nutritional Sciences, University of Morioka, Iwate 020-0694, Japan, +81-19-688-5555, E-mail: snarita@morioka-u.ac.jp

Tomoya Tsukazaki, Graduate School of Biological Sciences, Nara Institute of Science and Technology, Nara 630-0192, Japan, +81-74-372-5551, E-mail: ttsukazaki@mac.com

Keywords: peptidase family M48/ extracytoplasmic stress response/ σ^E pathway/ antibiotic resistance/ outer membrane

For Peer Review

31

For Peer Review

Summary

BepA (formerly YfgC) is an *Escherichia coli* periplasmic protein consisting of an N-terminal protease domain and a C-terminal tetratricopeptide repeat (TPR) domain. We have previously shown that BepA is a dual functional protein with chaperone-like and proteolytic activities involved in membrane assembly and proteolytic quality control of LptD, a major component of the outer membrane lipopolysaccharide translocon. Intriguingly, BepA can associate with the BAM complex: the β-barrel assembly machinery driving integration of β-barrel proteins into the outer membrane. However, the molecular mechanism of BepA function and its association with the BAM complex remains unclear. Here, we determined the crystal structure of the BepA TPR domain, which revealed the presence of two subdomains formed by four TPR motifs. Systematic site-directed *in vivo* photo-cross-linking was used to map the protein-protein interactions mediated by the BepA TPR domain, showing that this domain interacts both with a substrate and with the BAM complex. Mutational analysis indicated that these interactions are important for the BepA functions. These results suggest that the TPR domain plays critical roles in BepA functions through interactions both with substrates and with the BAM complex. Our findings provide insights into the mechanism of biogenesis and quality control of the outer membrane.

Introduction

Outer membrane proteins (OMPs) of Gram-negative bacteria play vital roles for the

For Peer Review

function of the outer membrane (OM), which acts as a barrier to hazardous compounds including a variety of chemicals and antibiotics (Nikaido, 2003). OMPs of Gram-negative bacteria, mitochondria, and chloroplasts are generally integrated into the OM as β-barrel structures (Misra, 2012). Following their synthesis (Pugsley, 1993), the insertion of bacterial OMPs into the OM is promoted by the β-barrel assembly machinery (BAM) complex (Noinaj *et al.*, 2017; Ricci & Silhavy, 2012). An essential component of this complex, BamA, has an OM-embedded β-barrel domain and periplasmic polypeptide transport-associated (POTRA) domains (Kim *et al.*, 2007). These POTRA domains each have a conserved β1-α1-α2-β2-β3 architecture, and have been suggested to interact with substrate OMPs via the β-strand augmentation mechanism (Kim *et al.*, 2007; Knowles *et al.*, 2008). In *Escherichia coli*, BamA has five POTRA domains and is associated with four lipoprotein subunits, BamB, C, D and E (Kim *et al.*, 2007; Malinverni *et al.*, 2006; Onufryk *et al.*, 2005; Ruiz *et al.*, 2005; Sklar *et al.*, 2007; Wu *et al.*, 2005).

Lipopolysaccharide (LPS) is another major component of the OM that is important for the OM structure and function (Nikaido, 2003). LptD is an OMP essential for *E. coli* growth (Braun & Silhavy, 2002), and forms a stable complex with the lipoprotein LptE to function in translocation of LPS to the outer leaflet of the OM (Freinkman *et al.*, 2011; Wu *et al.*, 2006). Correctly folded LptD ($LptD^{NC}$) that has been assembled into the OM possesses two pairs of non-consecutive (C31-C724 and C173-C725) disulfide bonds that connect the periplasmic and the β-barrel domains (Dong *et al.*, 2014; Kadokura *et al.*, 2004; Narita *et al.*, 2013; Qiao *et al.*, 2014; Ruiz *et al.*, 2010). These two disulfide bonds are formed by isomerization of disulfide bonds between successive pairs of cysteine residues (C31-C173 and C724-C725), which is likely triggered by association with LptE

For Peer Review

(Chng *et al.*, 2012; Narita *et al.*, 2013).

We have studied the function of β-barrel assembly-enhancing protease A (BepA; formerly called YfgC), a periplasmic M48 family peptidase homolog, and found that this protein facilitates the disulfide bond isomerization of LptD (Narita *et al.*, 2013). In the absence of BepA, OM assembly of LptD is retarded and an LptD assembly intermediate ($LptD^C$) with the consecutive disulfide bonds (C31-C173 and C724-C725) is accumulated in the periplasm (Narita *et al.*, 2013). Cells defective in the BepA function exhibit increased sensitivity to antibiotics such as erythromycin and rifampicin possibly due to compromised barrier functions of the OM (Narita *et al.*, 2013). BepA is also involved in proteolytic quality control of LptD; when the maturation of LptD was impaired by the depletion of LptE, accumulated $LptD^C$ was degraded in a BepA-dependent manner (Narita *et al.*, 2013). It has also been shown that misassembled BamA generated in Δ*surA* mutant cells undergoes BepA-dependent degradation (Narita *et al.*, 2013). These previous results suggested that BepA possesses both chaperone-like function that promotes the assembly of LptD and proteolytic functions that eliminate misassembled OMPs, and plays a critical role in maintaining the quality of the OM (Narita *et al.*, 2013; Soltes *et al.*, 2017). However, it is unclear how BepA promotes the assembly and degradation of OMPs and how these chaperone-like and proteolytic capacities of BepA are differentially activated depending on the folding state of OMPs, including LptD.

Sequence predictions suggest that BepA may have a C-terminal tetratricopeptide repeat (TPR) domain (The UniProt Consortium, 2017). TPR domains, which generally act in protein-protein interactions, comprise 3 to 16 repeats of 34 amino acids (TPR motifs), forming two anti-parallel α-helices packed in tandem arrays (D'Andrea & Regan,

For Peer Review

2003; Hirano *et al.*, 1990; Lamb *et al.*, 1995; Sikorski *et al.*, 1990; Zeytuni & Zarivach, 2012). Diverse cellular processes are controlled by proteins with TPR domains, including transcription, cell cycle control, protein translocation and protein degradation (Allan & Ratajczak, 2011). While multiple TPR motifs are predicted in BepA, the regions assigned as a TPR motif differ depending on the prediction methods (The UniProt Consortium, 2017; Karpenahalli *et al.*, 2007). In this study, we focused on determining the structure, function and protein-protein interactions mediated by the TPR domain of BepA to gain insights into the BepA function. The results of our systematic pBPA-mediated *in vivo* cross-linking and site-directed mutagenesis, informed by the crystal structure of the TPR domain presented here, explain how this domain plays an important role in BepA function through interaction with the BAM complex and substrate proteins.

Results

The TPR domain of BepA is required for its functionality

To examine whether the TPR domain is required for the BepA function, we constructed C-terminally truncated derivatives (Tr308-Tr472) by introducing an amber codon into several positions in the TPR domain (Fig. 1A). When expressed from a plasmid in Δ*bepA* cells, proteins of the expected sizes accumulated for Tr374 and Tr426 (Fig. 1A). Although expression of wild-type BepA suppressed phenotypes caused by the absence of BepA, that is, elevated erythromycin sensitivity and accumulation of $LptD^{C}$, expression of BepA(Tr374) and BepA(Tr426) did not (Fig. 1B and Supporting Information Fig. S1A). In addition, whereas a protease active site motif mutant of BepA, BepA(E137Q),

For Peer Review

dominant-negatively interfered with the functioning of the chromosomally-encoded wild-type protein, it lost the ability to cause dominant negative effects when C-terminally truncated (Fig. 1B and Supporting Information Fig. S1A). These results suggest that the TPR domain is important for BepA to function normally.

The BepA TPR domain consists of two subdomains formed by TPR modules

As a first step to understand the role of the TPR domain in the BepA function, we sought its structural information. Although the C-terminal region of BepA is predicted to contain several TPR motifs, it is difficult to predict the exact structure of the BepA TPR domain solely from the sequence information. We thus used X-ray crystallography to determine the structure of the BepA TPR domain (310–482) at 1.7 Å resolution with R_{work} = 16.8% and R_{free} = 19.9% (Fig. 2 and Table 1). The structure revealed that the BepA TPR domain is composed of ten α-helices (H1 to H10) arranged anti-parallel. Structural comparison using the Dali server (Holm & Laakso, 2016) showed that at least the N-terminal 3 helix-turn-helix regions (H1 to H6) of the BepA TPR domain appear to fit well with the TPR motifs of several other proteins such as the *Candidatus Magnetobacterium bavaricum* magnetosome-associated TPR-containing protein MamA (3vty_a: Zeytuni *et al.*, 2012) and human O-linked N-acetylglucosamine transferase (4n3a_a:Lazarus *et al.*, 2013). Analysis using the UniProt database (The UniProt Consortium, 2017) suggests that the H1/H2, H3/H4, H5/H6, and H8/H9 pairs are TPR motifs and H7 and H10 are non-TPR helices. In contrast, the TPRpred program (Karpenahalli *et al.*, 2007) suggested that only the H3/H4 pair is not a TPR motif. The H3/H4 and H8/H9 pairs contain residues matching the TPR motif consensus at 6 and 7, respectively, of the 8 positions, whereas the H7/H8 and H9/H10 pairs contain only 3 consensus residues. We decided to

For Peer Review

provisionally adopt the assignment by UniProt. Therefore, in this paper we refer to the H1/H2, H3/H4, H5/H6, and H8/H9 pairs as TPR1 to 4 with the odd-numbered and even-numbered helices called A and B helices, respectively. Helices 7 and 10 are referred to as non-TPR helix 1 and 2 (nTH1 and nTH2) (Fig. 2A and B). A C-terminal non-TPR helix, called a capping helix, is observed in many other TPR domains (Hirano *et al.*, 1990). The BepA TPR domain contains two subdomains. The N-terminal subdomain, which is composed of TPR1-3 and nTH1, forms a pocket architecture as frequently observed in other TPR domains. Its concave surface is negatively charged (Fig. 2B and C). In the crystal structure, the pocket is empty, whereas several previous studies have proven that similar pockets in TPR domains can be occupied by extended polypeptides (Allan & Ratajczak, 2011; D'Andrea & Regan, 2003; Zeytuni & Zarivach, 2012). TPR4 of BepA forms, in combination with TPR3B, nTH1, and nTH2, a C-terminal subdomain that has a small cavity that faces away from the pocket of the N-terminal subdomain.

The BepA TPR domain interacts with multiple BAM complex components

Because TPR domains are generally involved in protein-protein interactions, it seemed possible that the BepA TPR domain also interacts with other proteins. Previous studies showed that TPR domains interact with their partner proteins in several different manners; some interact with the convex surface of a TPR domain whereas others interact with the rims or the concave surfaces (Allan & Ratajczak, 2011; Zeytuni & Zarivach, 2012). We thus employed a systematic *in vivo* photo-cross-linking approach to identify possible interacting partners in an unbiased manner (Chin *et al.*, 2002; Chin & Schultz, 2002). This technique has been successfully applied to analysis of protein-protein interactions in a variety of biological processes (Choi *et al.*, 2014; Maklashina *et al.*,

For Peer Review

2016; Miyazaki *et al.*, 2016; Akiyama *et al.*, 2017; Shiota *et al.*, 2015; Freinkman *et al.*, 2011; Mori & Ito, 2006). Each codon for the 179 residues in the entire TPR domain (309 to 487) was changed to an amber codon by site-directed mutagenesis to allow suppressor tRNA-mediated incorporation of a nonnatural, photoreactive amino acid, p-benzoylphenylalanine (pBPA). Δ*bepA* cells expressing each of these pBPA-incorporated mutants were UV-irradiated to cause cross-linking with interacting proteins. SDS-PAGE and immunoblotting analysis of the whole cell proteins showed that many of the pBPA mutants apparently generated bands of larger sizes that were detected by anti-BepA antibody (Supporting Information Fig. S2). Among these pBPA mutants, 42 were picked up and examined further. We found that most of them generated bands of larger sizes in a UV-dependent manner, indicating that these bands represented crosslinked products (Fig. 3). A complementation assay indicated that these pBPA mutants, except BepA(N364pBPA), retained biological function because they restored erythromycin sensitivity of the Δ*bepA* strain (Supporting Information Fig. S3A, pBPA(+)). Note that mutants with an amber codon in the most C-terminal part complemented the Δ*bepA* mutation even in the absence of pBPA, suggesting that the C-terminal region after L477 is not essential for BepA function (Supporting Information Fig. S3A). From these results, we expected that some of the detected cross-linkings could reflect functional interactions of BepA with partner proteins.

We previously showed that BepA could be photo-cross-linked and chemically cross-linked to BamA (Narita *et al.*, 2013). In addition, BepA was co-isolated with the BAM complex in pull-down experiments (Narita *et al.*, 2013). These observations suggest that BepA interacts with the BAM complex. We thus examined whether the cross-linked products of the 42 TPR-pBPA mutants contained BamA, BamC, or BamD

For Peer Review

by immunoblotting with antibodies against the respective proteins. The results are summarized as follows: (i) cross-linking to BamA was detected for BepA having pBPA at A396, F404, Q428, or R480 (Supporting Information Fig. S4A); (ii) cross-linking to BamC was detected for BepA having pBPA at S451, S455, or L459 (Fig. 4B and Supporting Information Fig. S4B); and (iii) cross-linking to BamD was detected for BepA having pBPA at N323, D444, S448, S452, Q464, Q478, or K482 (Supporting Information Fig. S4C). We previously found that the efficiency of chemical cross-linking to the BAM components was significantly increased when BepA carried a protease active site motif mutation (E137Q) (Narita *et al.*, 2013). Use of the BepA(pBPA) proteins additionally having the E137Q mutation markedly increased the efficiencies of cross-linking to BamA (Fig. 4A and Supporting Information Fig. S4D), and also enabled the detection of cross-linking to BamA at several neighboring positions (N397, N400, S461, and L462) (Fig. 4A). The E137Q mutation also increased the pBPA-mediated cross-linking to BamD at N323 and S452, whereas it apparently decreased cross-linking at some other positions (Q464, Q478, and K482) (Fig. 4C).

We further analyzed the BepA-BAM interaction by conducting cross-linking experiments using BamA proteins having a pBPA substitution at several positions in the POTRA domain. After UV-irradiation of cells, the BamA derivatives were purified via an N-terminally-attached His_6-tag. Immunoblotting analysis with anti-BepA antibody revealed that BamA having pBPA at E224 in the POTRA3 domain generated a cross-linked adduct (Fig. 5A). Complementation assays suggested that the BamA(E224pBPA) mutant retains functionality (Supporting Information Fig. S3B). Importantly, E224 faces the inside of the periplasmic ring-like structure formed by the BamA POTRA domains and the other BAM components (Fig. 5B). Taken together with

For Peer Review

the results that the BepA TPR domain would directly interact with the BAM complex, it seems likely that the BepA TPR domain is inserted into the interior space of the periplasmic ring-like structure of the BAM complex (see Discussion and Fig. 9).

The BepA TPR domain is also involved in the interaction with LptD

The pBPA-mediated *in vivo* photo-cross-linking approach enables detection of not only stable but also transient protein-protein interactions, such as those with substrates (Chin *et al.*, 2002; Chin & Schultz, 2002). To identify the cross-linking partners of BepA, we selected 6 BepA derivatives having pBPA at N323, N364, F404, S455, K458, or S461 for which multiple and/or strong bands of cross-linked products were generated. After UV-irradiation, cells expressing a BepA(E137Q) derivative with a respective pBPA substitution were lysed and the BepA-derivatives were affinity-purified using a His_{10}-tag C-terminally attached to BepA (Supporting Information Fig. S5). Liquid chromatography-mass spectrometry (nano LC-MS/MS) analysis of the purified cross-linked products identified several candidates for BepA interactors (Table 2). Consistent with the immunoblotting results (Fig. 4A and C), BamD was detected with a high score for BepA(N323pBPA), and BamA was detected with high scores for BepA(F404pBPA) and BepA(S461pBPA). Notably, LptD was also detected for BepA(N323pBPA) and BepA(F404pBPA), although the scores were relatively low. Cross-linking of LptD to BepA(N323pBPA) and BepA(F404pBPA) was confirmed by anti-LptD immunoblotting analysis of the purified cross-linked products (Fig. 6A and B). Cross-linking of LptD to BepA was also enhanced by the E137Q mutation of BepA (Fig. 6A and B). These results suggest that the TPR domain of BepA is involved in interaction with LptD as well. Whereas the BepA(N323pBPA)-BamD adduct was formed

For Peer Review

248 independently of growth phase, the BepA(N323pBPA)-LptD adduct was detected in mid
249 to late log-phase cells, and not in overnight (~24 h) cultured cells (Fig. 6C).
250 In addition to the BAM components and LptD, three proteins (LoiP, OmpA, and
251 YdgA) were detected as possible cross-linking partners by mass spectrometry analysis
252 (Table 2). Among them, LoiP (YggG), an outer membrane lipoprotein homologous to
253 BepA, has been reported to interact with BepA (Lütticke *et al.*, 2012).
254
255 *Mapping of the cross-linked sites on the structure of the TPR domain*
256 We mapped the positions of the residues cross-linked to the BAM components (Fig.
257 4D) and LptD (Fig. 6D) on the crystal structure of the BepA TPR domain that we had
258 determined.
259 The BamA-cross-linking sites lie along TPR3B helix, at the N-terminal portion of
260 TPR4A helix, and on the N- and C-terminal portions of nTH2 helix, all facing the cavity.
261 This is in contrast to the BamD cross-linking sites, which were mapped to the TPR4B
262 and nTH2 helices and located on the convex surface of the cavity. The BamC
263 cross-linking sites reside in a region encompassing the C-terminal portion of the TPR4B
264 helix and the following L5 loop region. These observations suggest that BepA mainly
265 interacts with the BAM complex at the C-terminal subdomain of the TPR domain that
266 forms a small "cavity".
267 One (F404) of the two LptD-cross-linking sites was also mapped in the C-terminal
268 cavity-forming subdomain whereas the other (N323) is in the N-terminal subdomain that
269 forms a "pocket"; they are located in or near the loop regions on opposite sides. It may
270 thus be possible that both of the subdomains are involved in binding with LptD.
271

For Peer Review

A single amino-acid substitution in the TPR domain affects the function of BepA

To investigate the role of the TPR domain-mediated interaction with other proteins in the physiological function of BepA, we selected several residues at which cross-linking to the BAM components and LptD was observed and carried out mutational analysis (Fig. 7). We first constructed Ala-substituted mutants for these residues. The accumulation levels of the respective mutant proteins expressed from a plasmid in the Δ*bepA* cells were largely comparable to the wild-type protein (Fig. 7A). The Ala substitution mutations except F404A did not affect the BepA function, as the Δ*bepA* cells individually expressing these mutants exhibited erythromycin resistance comparable to those expressing the wild-type protein (Fig. 7A and Supporting Information Fig. S1B). The apparent lack of phenotypes of these BepA variants could be either because BepA-partner interactions are mediated by contacts at multiple positions in a redundant manner or because the contacts at these sites provide a limited contribution to the BepA function. In contrast, the erythromycin resistance of cells expressing the F404A mutant was significantly lower than that of the cells expressing wild-type BepA (Fig. 7A and Supporting Information Fig. S1B). In addition, while the wild-type and the other mutant proteins suppressed the accumulation of $LptD^{C}$, an assembly intermediate of LptD, in the Δ*bepA* cells, the F404A mutant did not (Fig. 7A). To further examine the functional importance of F404, it was mutated to other amino acid residues with different side chain properties. The results showed that BepA remained functional only when F404 had been replaced by another aromatic residue (Y or W) (Fig. 7B and Supporting Information Fig. S1B). We concluded that the TPR domain plays a critical role in the function of BepA to maintain the OM integrity through promotion of LptD biogenesis.

For Peer Review

F404 in the TPR domain of BepA is important for protein-protein interaction

We then examined the effects of F404 mutations on interaction of BepA with the BAM components and LptD. The F404G or F404Y mutation was introduced into BepA(Q428pBPA), BepA(L459pBPA), BepA(D444pBPA), and BepA(N323pBPA), which had each yielded a cross-linked product with BamA, BamC, BamD, and LptD, respectively. Cross-linking experiments with these "double" mutants showed that introduction of the F404G mutation, but not the F404Y mutation, greatly reduced the efficiency of their cross-linking to the respective partner proteins (Fig. 7C and Supporting Information Fig. S6).

BepA degrades LptD and BamA when their OM assembly is impaired under an LptE-depleted or a *surA*-deleted condition, respectively (Narita *et al.*, 2013). We found that some LptD underwent degradation when His_{10}-tagged LptD ($LptD_{His10}$) was overexpressed along with wild-type BepA in the Δ*bepA* cells (Fig. 8A). The observed degradation of $LptD_{His10}$ was dependent upon the proteolytic activity of BepA as no degradation product was detected without co-expression of BepA or with co-expression of proteolytically inactive BepA(E137Q), suggesting that some of overproduced LptD that had failed to form a complex with LptE was degraded by BepA. LptD degradation products also accumulated when BepA(F404Y) was co-expressed, but they accumulated in significantly reduced amounts with BepA(F404G) co-expression (Fig. 8A). Similarly, overexpression of wild-type BepA or BepA(F404Y), but not that of BepA(E137Q), in the Δ*bepA* Δ*surA* cells, resulted in a decreased level of full-length BamA and concomitant accumulation of BamA degradation products. In contrast, expression of BepA(F404G) or BepA(F404D) exerted only marginal effects on BamA stability (Fig. 8B). These results suggest that F404 of BepA is an important residue, not only for

For Peer Review

interactions with the BAM components and LptD in LptD biogenesis, but also for the degradation of misassembled BamA and LptD.

We previously found that the C-terminally attached polyhistidine-tag of BepA is cleaved within the tag sequence (Narita *et al.*, 2013). As this cleavage was not observed for the E137Q mutant, even upon co-expression of the proteolytically active BepA (Fig. 8C), the truncation seems to be a result of self-cleavage. We found that the F404G mutation had little effect on the self-cleavage (Fig. 8D), although it significantly reduced the degradation of misassembled BamA and LptD. These results suggest that the F404G mutation would not inhibit the BepA's intrinsic protease activity. It is thus likely that the defective degradation of the substrate proteins (misassembled BamA and LptD) by BepA(F404G) results from impaired interaction of BepA with these proteins.

Discussion

We have previously shown that the periplasmic protein BepA, an M48 family peptidase homologue, is involved in biogenesis and quality control of LptD, the major subunit of the outer membrane LPS translocon (Narita *et al.*, 2013). We have also demonstrated that BepA can be associated with the BAM complex that catalyzes OMP assembly (Narita *et al.*, 2013). However, it remained unclear how BepA achieves these biological functions. Here we determined the structure of the isolated TPR domain and conducted systematic *in vivo* photo-cross-linking and mutagenesis analyses targeted to the TPR domain of BepA. Our results collectively elucidated the importance of the TPR domain in BepA function.

For Peer Review

Our previous results suggested that BepA interacts with components of the BAM complex (Narita *et al.*, 2013). Here, we showed that the TPR domain of BepA was cross-linkable to these BAM components in addition to LptD, providing evidence that BepA directly interacts with these proteins through its TPR domain. We found that pBPA at F404 in the BepA TPR domain can be cross-linked either to BamA or LptD, and that alterations of this residue impaired the normal functioning of BepA, suggesting that the TPR mediated interaction with either or both of these proteins is important for the BepA functions.

Cross-link adducts with BAM components were more prominent than those with LptD. Moreover, cross-linking to LptD, but not to BamD, was growth phase-dependent, and not detected in cells in stationary phase (Fig. 6C). The observed BepA-LptD cross-linking may reflect transient interaction of BepA with a newly synthesized LptD as a substrate, whereas BepA-BamD cross-linking may result from a more stable association of BepA with the BAM complex.

In addition to the BAM components and LptD, LoiP, YdgA, and OmpA were detected as possible cross-linked partners (Table 2). LoiP, an OM-associated lipoprotein protease homologous to BepA, has previously been shown to interact with BepA (Lütticke *et al.*, 2012). Although physiological function of LoiP is not known, absence of BepA weakens association of LoiP with the OM (Lütticke *et al.*, 2012). Partial membrane localization of BepA (Narita *et al.*, 2013) might at least partly be ascribed to its TPR domain-mediated interaction with LoiP. Physical or functional interaction of BepA with YdgA, a putative periplasmic protein with unknown function, and OmpA, one of the major OMPs, have not previously been reported. Because OmpA is a very abundant protein and its assembly is mediated by the BAM complex, the observed

For Peer Review

368 cross-linking of BepA with OmpA might not reflect their direct interaction, but result
369 from proximal localization of these proteins at the BAM complex. We also detected a
370 number of cross-linked products that were not reactive with antibodies to the BAM
371 components or LptD, raising the possibility that BepA interacts with additional proteins
372 (Fig. 3, Table 2 and Supporting Information Fig. S2). Identification of these proteins,
373 which might lead to the discovery of new substrates and/or co-operating cellular factors,
374 also awaits future study. The increased efficiencies of cross-linking when BepA carried
375 the E137Q mutation in the protease active site motif might suggest that the protease
376 active site region also participates in protein-protein interactions or that the protease
377 activity of BepA indirectly affects the interactions through proteolysis of some substrate
378 proteins.

379 We determined the crystal structure of the isolated TPR domain, which revealed that
380 it has four tandemly aligned TPR motifs. The tandemly aligned TPR motifs generally
381 form a superhelix with a single groove (concave) as a whole (Zeytuni & Zarivach, 2012).
382 In contrast, The TPR domain of BepA is composed of two palm-like structures with their
383 grooves facing opposite sides (see Results). The sites for cross-linking to BamA, BamC
384 and BamD were mostly mapped in the small palm region; the BamA cross-linking sites
385 were located in the cavity whereas the BamC and BamD cross-linking sites were located
386 on the convex surface with the exception of N323, a BamD cross-linking site that resides
387 within the loop between TPR1A and 1B helices in the larger palm. In contrast, most of
388 the sites in the larger palm at which cross-linking to unidentified proteins was observed
389 were mapped in the convex surface formed by the B-helices and the inter-helix loop
390 regions (Supporting Information Fig. S7). It is interesting that the many residues in the
391 convex surfaces of the BepA TPR domains probably participate in interactions with other

For Peer Review

proteins, whereas super-helix-forming canonical TPR domains usually interact with ligands via A helices forming concave surfaces (Blatch & Lässle, 1999; Scheufler *et al.*, 2000). It is, however, possible that some proteins that eluded the pBPA-mediated cross-linking interact with BepA at the concave surface of the larger palm.

Crystal structures of subunits of the BAM complex and the holo-complex show that the periplasmic POTRA domains of BamA form a ring-like architecture with the other BAM components (Bakelar *et al.*, 2016; Gu *et al.*, 2016; Han *et al.*, 2016). The periplasmic units appear to rotate with respect to the membrane-embedded barrel of BamA, to facilitate the insertion of substrate OMPs into the OM (Gu *et al.*, 2016; Han *et al.*, 2016). E224 of BamA is located in the POTRA3 domain and exposed to the interior of the periplasmic ring-like structure formed by the POTRA domains of BamA and the other BAM components. Our results that pBPA at E224 of BamA can be cross-linked to BepA suggest that BepA interacts with the BAM complex within the periplasmic ring-like structure. In addition, the smaller palm of the BepA TPR domain would interact with BamA, C and D (Fig. 4D). These appear to be achieved if we assume that the TPR domain of BepA can interact with the BAM complex by inserting into the interior of the ring-like structure. We manually docked the crystal structures of the BepA TPR domain and the BAM complex to construct a conceptual model of their association (Fig. 9A-C). In this model, the smaller palm region of the BepA TPR comes close to POTRA1 and POTRA5 of BamA, a central region of BamD, and an N-terminal region of BamC, which fits well with the interactions between the BepA TPR and the individual BAM components that were suggested from the cross-linking results. However, E224 of BamA, which was cross-linked to BepA, is located distantly from the BepA TPR. Additionally, N323 of the BepA TPR, which was cross-linked to BamD, appears to be too far from

For Peer Review

BamD to cross-link. The proposed structural flexibility of the BAM complex, including possible conformational changes in the BamA POTRA domains, might allow these resides to reach their respective cross-linking partners (Warner *et al.*, 2017; Fleming *et al.*, 2016; Iadanza *et al.*, 2016). Alternatively, BepA might interact with the BAM complex in several different configurations. If this mode of association is correct, the large protease domain (~30 kDa) of BepA would not be able to be simultaneously inserted into the ring-like structure, without a large conformational change in the periplasmic domain of the BAM complex.

What role does BepA play in the BAM-dependent assembly of LptD into the OM? It is possible that BepA binds the assembly intermediate of LptD, $LptD^{C}$, in the periplasm and targets it to the BAM complex in the OM (Fig. 10A) or that BepA first binds to the BAM complex where it accepts $LptD^{C}$ (Fig. 10B). In either case, BepA mediates productive transfer of LptD to the BAM complex to promote its efficient association with LptE and final assembly into the OM, although at present it cannot be ruled out that LptD interacts with the BAM complex before its association with BepA. When proper assembly of LptD is impaired, for example, due to reduced availability of LptE (Narita *et al.*, 2013), LptD ($LptD^{C}$) is retargeted for degradation, in which TPR-mediated interaction of BepA with the substrate is also required. Soltes *et al.* (2017) recently showed that BepA degrades a partially folded LptD variant (LptD4213) that is stalled at the BAM complex, which would mimic a late step assembly intermediate, but does not degrade LptD that has accumulated at an earlier step of assembly. These findings appear to fit more with the second model (Fig. 10B), although it would be also possible that BepA interacts with a substrate early on but degrade it after they have been targeted to the BAM complex.

For Peer Review

Our results showed that pBPA at N323 of BepA is cross-linkable to both LptD and BamD and that F404 is important for the interaction of BepA with BamA and LptD, and for the maturation of LptD. These residues might act as switches to facilitate the transfer of LptD between BepA and the BAM complex during assembly. More detailed kinetic studies of LptD assembly and its interactions with BepA and the BAM complex (and also with other cellular factors such as periplasmic chaperones), as well as structural information on the BepA-BAM and BepA-LptD complexes will be needed to fully understand the roles of BepA in the biogenesis and quality control of LptD and other OMPs.

Experimental Procedures

Bacterial strains and media

E. coli K12 strains and plasmids used in this study are listed in Supporting Information Table S1. Unless indicated otherwise, cells were grown in liquid or on solid L medium (containing 10 g l^{-1} Bacto Tryptone, 5 g l^{-1} yeast extract, and 5 g l^{-1} NaCl; pH was adjusted to 7.2 using NaOH) or M9 medium without $CaCl_2$ supplemented with 20 μg ml^{-1} of each of 19 amino acids other than methionine, 2 μg ml^{-1} thiamine, and 0.2% maltose. Unless otherwise specified, ampicillin (50 or 100μg ml^{-1}), chloramphenicol (20 or 50 μg ml^{-1}), kanamycin (30 μg ml^{-1}), or spectinomycin (50 μg ml^{-1}) were added for selecting transformants and for growing plasmid-harboring strains.

Plasmids

Plasmids used in this study are also listed in Supporting Information Table S1.

For Peer Review

Derivatives of pUC-bepA and pUC-bepA-his_{10} encoding a mutant form of BepA were constructed by site-directed mutagenesis using pairs of complementary primers. Derivatives of pUC-bepA(E137Q) and pUC-bepA(E137Q)-his_{10} encoding a double or triple mutant form of BepA(E137Q) were constructed similarly. pTnT-bamA was constructed as follows. A DNA fragment for the bamA gene with a 500 bp promoter region and a 40 bp terminator region was PCR-amplified using a pair of primers BglIIBamA-f (5'-GAAGATCTAATGGTAAAGCGATTGGTTTTGTCGGTATTGAGCCGAAAG-3') and BamASalI-r (5'-CCGGTCGACTCATCGCTACACTACCACTACATTCCTTTGTGGAGAACAC-3') from the genomic DNA of Escherichia coli MG1655. The amplified DNA fragment was digested with BglII and SalI and cloned into the BglII/SalI site of pTnT. pTnT-H6A2bamA encoding $_{His6}$BamA was constructed by site-directed mutagenesis of pTnT-bamA using a pair of primer BamANHis6A2-f (5'-CACCGTATACGGTGCTAGCCACCACCACCACCACCACGCGGCGGAAGGGT TCGTAGTGAA-3') and BamANHis6A2-r (5'-TTCACTACGAACCCTTCCGCCGCGTGGTGGTGGTGGTGGCTAGCACC GTATACGGTG-3'). pTnT H6A2bamA derivative encoding an amber mutant form of BamA were constructed by site-directed mutagenesis using pairs of complementary primers. pTTQ-lptD-his_{10} was constructed as follows. An lptD-his_{10} fragment was PCR-amplified from the genome of MC4100 using a pair of primers, lptD-his-for (5'-CGCGGGATCCCAACGTTACCGATGATGGAAC-3') and lptD-his-rev (5'-CGCGAAGCTTTCAATGATGATGATGATGATGATGATGATGCAAAGTGT TTTGATACGGCAG-3'), digested with BamHI and HindIII, and cloned into the same

For Peer Review

site of pTTQ18. pTWV-lptD-his$_{10}$ was constructed by subcloning the BamHI-HindIII fragment of pTTQ-lptD-his$_{10}$ into the same site of pTWV228. For construction of the pSTD-bepA plasmid and its derivatives, the EcoRI-HindIII bepA fragments of pUC-bepA and its derivatives encoding a mutant BepA were subcloned into the same sites of pSTD689. pNAS310 encoding the BepA TPR domain was constructed as follows. DNA fragment encoding residue 310-482 of BepA was amplified by PCR from pUC-bepA-his$_{10}$ using a pair of primers, TPR310 (5'-CGGGATCCGCAGCACAATATGGTCGTG-3') and TPR482r (5'-CCGCTCGAGTTACTTAAAGCGTTCCTGCAGC-3'). The amplified DNA fragment was digested with BamHI and XhoI and then cloned into the same sites of pET-16b-TEV, which is a modified version of the pET-16b (Novagen) expression vector in which the Factor Xa-cleavage site has been replaced by a tobacco etch virus (Tev) protease cleavage site. pNAS310(L450M) encoding the L450M mutant form of BepA were constructed by site-directed mutagenesis using pairs of complementary primers from pNAS310.

Purification of Se-Met labeled BepA TPR domain

pNAS310(L450M), a pET-based plasmid expressing MG–H$_{10}$–SSGENLYFQGS–BepA$_{310–482}$(L450M) was introduced into E. coli strain KRX cells (Promega). After cultivation of cells at 37°C to an A_{600} of approximately 0.5 in salt medium (containing 19 amino acids, 25 μg ml^{-1} Se-Met, 1mM isopropyl β-D-1-thiogalactopyranoside (IPTG), and 50 μg ml^{-1} ampicillin (Tsukazaki *et al.*, 2006), the protein expression was induced with 0.2% rhamnose at 17°C for 16 h. The cells were harvested by centrifugation (5,000 × g, 15 min), suspended in Buffer A [20 mM Tris-HCl (pH 7.0), 500 mM NaCl, 20 mM

For Peer Review

imidazole (pH 7.0), 1 mM 2-mercaptoethanol (ME), 0.1 mM phenylmethanesulfonyl fluoride (PMSF) and 0.002% n-dodecyl-D-maltoside] and disrupted by sonication. After centrifugation (12,000 × g, 40 min), the supernatant was mixed with Ni-NTA Agarose (QIAGEN) equilibrated with Buffer A. The resin was washed with Buffer A and eluted with Buffer B [20 mM Tris-HCl (pH 7.0), 500 mM NaCl, 300 mM imidazole (pH 7.0), 1 mM ME, 0.1 mM PMSF and 0.002% n-dodecyl-D-maltoside]. The eluate was dialyzed against Buffer C [20 mM Tris-HCl (pH 7.0), 500 mM NaCl, 1 mM ME, 0.1 mM PMSF and 0.002% n-dodecyl-D-maltoside]. During dialysis, the N-terminal tag of the TPR domain was cleaved using TEV protease (1/20 ratio by weight) for 16 h. The solution containing the cleaved sample [Se-Met labeled GS–$BepA_{310–482}$(L450M)] was mixed with Ni-NTA Agarose equilibrated with Buffer A. The flow-through sample was concentrated using an Amicon Ultra 3K filter (Millipore) and loaded on a Superdex 200 Increase column (GE Healthcare) equilibrated with Buffer C. The concentrations of protein and buffer were adjusted using an Amicon Ultra 3K filter to 10 mg ml^{-1} BepA TPR, 20 mM Tris-HCl (pH 7.0), 260 mM NaCl, 1 mM ME, 0.1 mM PMSF, and 0.002% n-dodecyl-D-maltoside.

Crystallization, data collection, and structure determination

A volume of 0.1 µl of 20 mg ml^{-1} purified Se-Met-labeled BepA TPR domain was mixed with 0.1 µl of reservoir solution [32% polyethylene glycol (PEG) 4000, 90 mM sodium citrate (pH 5.9), 180 mM ammonium acetate, 5 mM KH_2PO_4, and 2% PEG 8000]. The drop was incubated at 20°C according to the sitting drop vapor diffusion method against the reservoir solution additionally containing approximately 200 mM NaCl. The best rhombohedral shaped crystals grew to dimensions of 80 × 80 × 80 µm.

For Peer Review

The structure of the BepA TPR domain was determined by multi-wavelength anomalous dispersion (MAD). The X-ray diffraction data were collected at Photon Factory beamline BL-1A with three-wavelength values of 0.9787 (peak), 0.9794 (edge), and 0.9900 Å (low-energy remote) and were processed using HKL2000 (HKL Research Inc.). Identification of initial Se sites and initial model building were accomplished using SHELXC/D/E (Sheldrick, 2010). The model was reformed and refined using Coot (Emsley & Cowtan, 2004) and PHENIX.refine (Afonine *et al.*, 2012) for the peak dataset. To reduce the model bias and improve the phases, simulated annealing refinement was performed at an early stage of the model building, followed by several cycles of positional refinement combined with individual B-factor refinement. Finally, the structure of Se-Met-labeled BepA TPR domain (GS–$BepA_{310–482}$) was refined to R-work = 16.1% and R-free = 18.8% at 1.7 Å resolution. The refinement statistics are summarized in Table 1. All residues in the final models were found in the allowed regions of the Ramachandran plots calculated with MolProbity (Chen *et al.*, 2010). The crystal contains one molecule in the asymmetric unit. The atomic coordinates and structure factors have been deposited in the Protein Data Bank, under the accession code 5XI8. The molecular graphics were illustrated with CueMol2 (http://www.cuemol.org/).

Photo-cross-linking of pBPA-containing BepA and BamA

SN56 cells carrying pEVOL-pBpF and a pUC-bepA-his_{10} derivative with an amber mutation were grown at 30°C to late log phase (at 0.6-0.7 units with TAITEC OD monitor) in L or M9 medium supplemented with 0.2% arabinose, 1 mM IPTG, 1 mM pBPA (Bachem) and appropriate antibiotics. Cultures were chilled on ice for 10 min and a 250 µl portion was UV-irradiated at 365 nm in a petri dish for 10 min by using a

For Peer Review

B-100AP UV lamp (UV Products) at a distance of 4 cm. Proteins were then precipitated by the addition of an equal volume of 10% (w/v) trichloroacetic acid, solubilized in SDS sample buffer and subjected to SDS-PAGE and immunoblotting. For analysis of membrane fractions from UV-irradiated cells, 2 ml of culture was UV-irradiated. After washing and resuspending with 10 mM Tris-HCl (pH 8.1), cells were disrupted by sonication. Following the removal of unbroken cells by centrifugation at 10,000 × g for 5 min, membranes were collected by ultracentrifugation at 100,000 × g for 60 min and resuspended in 10 mM Tris-HCl (pH 8.1). Proteins were precipitated with trichloroacetic acid and subjected to SDS-PAGE and immunoblotting.

Cross-linking of pBPA-containing BamA was conducted as follows. Cells of the BamA depletion strain (Lehr *et al.*, 2010), carrying pSup-BpaRS-6TRN and a pTnT-H6A2bamA(amber mutant) that expresses a $_{His6}$BamA derivative from the native *bamA* promoter, were grown at 37°C to stationary phase (at OD_{600}=1.5-1.8) in L medium supplemented with 0.2% glucose, 1 mM pBPA and appropriate antibiotics. A 25-ml portion of the culture was UV-irradiated at 365 nm in a petri dish for 10 min at a distance of 3 cm. Cells were solubilized with 1% SDS buffer [50 mM Tris-HCl (pH 8.1), 150 mM NaCl, 1% SDS] and then diluted five-fold with 0.5% Triton X-100 buffer [50 mM Tris-HCl (pH 8.1), 150 mM NaCl, 0.5% Triton X-100]. His_6-BamA and its cross-linked products were affinity purified by Ni-NTA agarose chromatography. They were eluted with Elution Buffer [50 mM Tris-HCl (pH 8.1), 150 mM NaCl, 0.5% Triton X-100, 400 mM imidazole]. Proteins in the eluates were acid-precipitated and analyzed by SDS-PAGE and immunoblotting.

Purification of BepA cross-linked products

For Peer Review

584 UV-irradiated cells from a 25-ml culture were harvested, washed with 10 mM
585 Tris-HCl (pH 8.1) and disrupted by sonication in the same buffer. After the removal of
586 unbroken cells by centrifugation at 10,000 × g for 5 min, membranes were collected by
587 ultracentrifugation at 100,000 × g for 60 min. Membranes were solubilized with 1% SDS
588 buffer [50 mM Tris-HCl (pH 8.1), 150 mM NaCl, 1% SDS] and centrifuged at 10,000 ×
589 g for 5 min. Supernatants were 10-fold diluted with buffer containing 50 mM Tris-HCl
590 (pH 8.1) and 150 mM NaCl, mixed with TALON metal affinity resin (Clontech) and
591 rotated slowly for 2 h at room temperature. Resin was extensively washed with Binding
592 Buffer [50 mM Tris-HCl (pH 8.1), 150 mM NaCl, 0.1% SDS], and finally bound
593 proteins were eluted with 500 µl of Elution Buffer [50 mM Tris-HCl (pH 8.1), 150 mM
594 NaCl, 0.1% SDS, 81 mM EDTA]. Purified preparations of BepA cross-linked products
595 were approximately 20-30-fold concentrated using Amicon Ultra 0.5 30K centrifugal
596 filters (Millipore) at 14,000 × g for 15 min. Concentrated samples were mixed with an
597 equal volume of 2× SDS-sample buffer with a final concentration of 10% (w/v) ME.
598
599 *Mass spectrometry*
600 Purified cross-linked products containing BepA were visualized by silver staining
601 after SDS-PAGE. An excised silver-stained gel band was destained with destaining
602 solution in the Silver Stain MS Kit (Wako Pure Chemical Industries) and then dried in
603 vacuo. The band was incubated with 0.01 µg of N-tosyl-L-phenylalanine chloromethyl
604 ketone (TPCK)-treated trypsin (Worthington Biochemical Corporation) in 10 mM
605 Tris-HCl (pH 8.1) at 37°C for 12 h. An aliquot of the digest was analyzed by nano
606 LC-MS/MS using a Q Exactive™ Hybrid Quadrupole-Orbitrap Mass Spectrometer
607 (Thermo Fisher Scientific). The peptides were separated using a nano-spray column

For Peer Review

608 NTCC-360/75-3-105 (0.075 mm I.D. ×105 mm L, particle diameter 3 μm, Nikkyo
609 Technos) at a flow rate of 300 nL/min. The mass spectrometer was operated in the
610 positive-ion mode, and the spectra were acquired in a data-dependent TOP 10 MS/MS
611 method. The MS/MS spectra were searched against the NCBInr 20151005 database
612 (Taxonomy: Escherichia coli, 1436264 sequences) using an in-house MASCOT server
613 (version: 2.5; Matrix Science).
614
615 *Determination of minimum inhibitory concentration (MIC)*
616 For determination of MIC of erythromycin, overnight cultures were diluted 10^3-fold
617 with L-medium and 5 μl were inoculated on L medium-based agar plates supplemented
618 with 0, 1.56, 2.2, 3.13, 4.4, 6.25, 8.8, 12.5, 17.5, 25, 35, 50, and 70 μg ml^{-1} erythromycin.
619 The plates were incubated for 18-20 h at 30 °C.
620
621 *Materials and other techniques*
622 SDS-PAGE and immunoblotting were carried out essentially as described (Laemmli,
623 1970; Shimoike *et al.*, 1995), unless otherwise specified. Penta-His HRP Conjugate
624 (QIAGEN) was used to probe polyhistidine-tagged proteins. For visualization of proteins
625 in immunoblotting, ECL or ECL Prime Western Blotting Detection Reagent (GE
626 Healthcare) and detection was done using a lumino-image analyzer (LAS-4000mini;
627 Fujifilm) or X-ray film. TAITEC mini photo 518R (TAITEC) was used to monitor cell
628 density in the cross-linking assay of pBPA-containing BepA.
629
630
631 **Acknowledgements**

For Peer Review

We thank Yohei Hizukuri and Eiji Ishii for stimulating discussion and Michiyo Sano and Akito Yoshimi for technical support. We are grateful to Shin-ichi Matsuyama, Hajime Tokuda, Osamu Nureki, Ingo B. Autenrieth, and Thomas J. Silhavy for bacterial strains, plasmids and antisera. This work was supported by JSPS KAKENHI Grant Numbers JP15H04350 (to Y.A.), JP15K07008 (to S.N.), and JP26291023 (to. T.T.), MEXT KAKENHI Grant Numbers JP15H01532 (to Y.A.), JP26119007 (to. T.T.), JP17H05669 (to Y.T.) and JP15H01537 (to Y.T.), and the research grants from Asahi Glass Foundation (to S.N.). This work was also supported by Platform for Drug Discovery, Informatics, and Structural Life Science funded by the Ministry of Education, Culture, Sports, Science and Technology, Japan (to. T.T.) and Australian Research Council Discovery Project Grant DP160100227 (to T.L.). The authors declare that they have no conflicts of interest with the contents of this article.

Author Contributions

YD, HM, SN, YA, TS (T. Shiota), and TL conceived the idea and designed the experiments. YD, CI, YT, HS, TT, TS (T. Shiota), TL, TS (T. Suziuki), ND and RM performed experiments. YD, RM, TS (T. Shiota), TL, ND, TT, SN, and YA wrote the paper.

References

For Peer Review

656

657 Afonine, P.V., R.W. Grosse-Kunstleve, N. Echols, J.J. Headd, N.W. Moriarty, M. Mustyakimov,
658 *et al.* (2012) Towards automated crystallographic structure refinement with phenix.refine.
659 *Acta Crystallogr D Biol Crystallogr* **68**: 352-367.

660 Akiyama, K., Y. Hizukuri and Y. Akiyama (2017) Involvement of a conserved GFG motif region
661 in substrate binding by RseP, an Escherichia coli S2P protease. *Mol Microbiol* **104**:
662 737-751.

663 Allan, R.K. and T. Ratajczak (2011) Versatile TPR domains accommodate different modes of
664 target protein recognition and function. *Cell Stress Chaperones* **16**: 353-367.

665 Bakelar, J., S.K. Buchanan and N. Noinaj (2016) The structure of the β-barrel assembly
666 machinery complex. *Science* **351**: 180-186.

667 Blatch, G.L. and M. Lässle (1999) The tetratricopeptide repeat: a structural motif mediating
668 protein-protein interactions. *BioEssays* **21**: 932–939.

669 Braun, M. and T.J. Silhavy (2002) Imp/OstA is required for cell envelope biogenesis in
670 *Escherichia coli*. *Mol Microbiol* **45**: 1289-1302.

671 Chen, V.B., W.B. Arendall, 3rd, J.J. Headd, D.A. Keedy, R.M. Immormino, G.J. Kapral, *et al.*
672 (2010) MolProbity: all-atom structure validation for macromolecular crystallography.
673 *Acta Crystallogr D Biol Crystallogr* **66**: 12-21.

674 Chin, J.W., A.B. Martin, D.S. King, L. Wang and P.G. Schultz (2002) Addition of a
675 photocrosslinking amino acid to the genetic code of *Escherichia coli*. *Proc Natl Acad Sci*
676 *U S A* **99**: 11020-11024.

677 Chin, J.W. and P.G. Schultz (2002) *In vivo* photocrosslinking with unnatural amino acid
678 mutagenesis. *ChemBioChem* **3**: 1135-1137.

679 Chng, S.S., M. Xue, R.A. Garner, H. Kadokura, D. Boyd, J. Beckwith, *et al.* (2012) Disulfide

For Peer Review

680 rearrangement triggered by translocon assembly controls lipopolysaccharide export.
681 *Science* **337**: 1665-1668.
682 Choi, K.Y., J.M. Spencer and N.L. Craig (2014) The Tn7 transposition regulator TnsC interacts
683 with the transposase subunit TnsB and target selector TnsD. *Proc Natl Acad Sci U S A*
684 **111**: E2858-2865.
685 D'Andrea, L.D. and L. Regan (2003) TPR proteins: the versatile helix. *Trends Biochem. Sci.* **28**:
686 655-662.
687 Dong, H., Q. Xiang, Y. Gu, Z. Wang, N.G. Paterson, P.J. Stansfeld*, et al.* (2014) Structural basis
688 for outer membrane lipopolysaccharide insertion. *Nature* **511**: 52-56.
689 Emsley, P. and K. Cowtan (2004) Coot: model-building tools for molecular graphics. *Acta*
690 *Crystallogr D Biol Crystallogr* **60**: 2126-2132.
691 Fleming, P.J., D.S. Patel, E.L. Wu, Y. Qi, M.S. Yeom, M.C. Sousa*, et al.* (2016) BamA POTRA
692 domain interacts with a native lipid membrane surface. *Biophys J* **110**: 2698-2709.
693 Freinkman, E., S.S. Chng and D. Kahne (2011) The complex that inserts lipopolysaccharide into
694 the bacterial outer membrane forms a two-protein plug-and-barrel. *Proc Natl Acad Sci U*
695 *S A* **108**: 2486-2491.
696 Gu, Y., H. Li, H. Dong, Y. Zeng, Z. Zhang, N.G. Paterson*, et al.* (2016) Structural basis of outer
697 membrane protein insertion by the BAM complex. *Nature* **531**: 64-69.
698 Han, L., J. Zheng, Y. Wang, X. Yang, Y. Liu, C. Sun*, et al.* (2016) Structure of the BAM complex
699 and its implications for biogenesis of outer-membrane proteins. *Nature Struct Mol Biol*
700 **23**: 192-196.
701 Hirano, T., N. Kinoshita, K. Morikawa and M. Yanagida (1990) Snap helix with knob and hole:
702 essential repeats in *S. pombe* nuclear protein *nuc2*$^{+}$. *Cell* **60**: 319-328.
703 Holm, L. and L.M. Laakso (2016) Dali server update. *Nucleic Acids Res* **44**: W351-355.

For Peer Review

Iadanza, M.G., A.J. Higgins, B. Schiffrin, A.N. Calabrese, D.J. Brockwell, A.E. Ashcroft, *et al.* (2016) Lateral opening in the intact β-barrel assembly machinery captured by cryo-EM. *Nat Commun* **7**: 12865.

Kadokura, H., H. Tian, T. Zander, J.C.A. Bardwell and J. Beckwith (2004) Snapshots of DsbA in action: Detection of proteins in the process of oxidative folding. *Science* **303**: 534-537.

Karpenahalli, M.R., A.N. Lupas and J. Söding (2007) TPRpred: a tool for prediction of TPR-, PPR- and SEL1-like repeats from protein sequences. *BMC Bioinformatics* **8**: 2.

Kim, S., J.C. Malinverni, P. Sliz, T.J. Silhavy, S.C. Harrison and D. Kahne (2007) Structure and function of an essential component of the outer membrane protein assembly machine. *Science* **317**: 961-964.

Knowles, T.J., M. Jeeves, S. Bobat, F. Dancea, D. McClelland, T. Palmer, *et al.* (2008) Fold and function of polypeptide transport-associated domains responsible for delivering unfolded proteins to membranes. *Mol Microbiol* **68**: 1216-1227.

Laemmli, U.K. (1970) Cleavage of structural proteins during the assembly of the head of bacteriophage T4. *Nature* **227**: 680-685.

Lamb, J.R., S. Tugendreich and P. Hieter (1995) Tetratrico peptide repeat interactions: to TPR or not to TPR? *Trends Biochem Sci* **20**: 257-259.

Lazarus, M.B., J. Jiang, V. Kapuria, T. Bhuiyan, J. Janetzko, W.F. Zandberg, *et al.* (2013) HCF-1 is cleaved in the active site of O-GlcNAc transferase. *Science* **342**: 1235-1239.

Lehr, U., M. Schutz, P. Oberhettinger, F. Ruiz-Perez, J.W. Donald, T. Palmer, *et al.* (2010) C-terminal amino acid residues of the trimeric autotransporter adhesin YadA of *Yersinia enterocolitica* are decisive for its recognition and assembly by BamA. *Mol Microbiol* **78**: 932-946.

Lütticke, C., P. Hauske, U. Lewandrowski, A. Sickmann, M. Kaisera and M. Ehrmann (2012) *E.*

For Peer Review

coli LoiP (YggG), a metalloprotease hydrolyzing Phe-Phe bonds. *Mol Biosyst* **8**: 1775-1782.

Maklashina, E., S. Rajagukguk, C.A. Starbird, W.H. McDonald, A. Koganitsky, M. Eisenbach*, et al.* (2016) Binding of the covalent flavin assembly factor to the flavoprotein subunit of complex II. *J Biol Chem* **291**: 2904-2916.

Malinverni, J.C., J. Werner, S. Kim, J.G. Sklar, D. Kahne, R. Misra*, et al.* (2006) YfiO stabilizes the YaeT complex and is essential for outer membrane protein assembly in *Escherichia coli*. *Mol Microbiol* **61**: 151-164.

Misra, R. (2012) Assembly of the β-barrel outer membrane proteins in Gram-negative bacteria, mitochondria, and chloroplasts. *ISRN Mol Biol* **2012**: 708203.

Miyazaki, R., T. Yura, T. Suzuki, N. Dohmae, H. Mori and Y. Akiyama (2016) A novel SRP recognition sequence in the homeostatic control region of heat shock transcription factor σ^{32}. *Sci Rep* **6**: 24147.

Mori, H. and K. Ito (2006) Different modes of SecY-SecA interactions revealed by site-directed *in vivo* photo-cross-linking. *Proc Natl Acad Sci U S A* **103**: 16159-16164.

Narita, S., C. Masui, T. Suzuki, N. Dohmae and Y. Akiyama (2013) Protease homolog BepA (YfgC) promotes assembly and degradation of β-barrel membrane proteins in *Escherichia coli*. *Proc Natl Acad Sci U S A* **110**: E3612-3621.

Nikaido, H. (2003) Molecular basis of bacterial outer membrane permeability revisited. *Microbiol Mol Biol Rev* **67**: 593-656.

Noinaj, N., J.C. Gumbart and S.K. Buchanan (2017) The β-barrel assembly machinery in motion. *Nature Rev Microbiol* **15**: 197-204.

Onufryk, C., M.L. Crouch, F.C. Fang and C.A. Gross (2005) Characterization of six lipoproteins in the σ^{E} regulon. *J Bacteriol* **187**: 4552-4561.

For Peer Review

752 Pugsley, A.P. (1993) The complete general secretory pathway in gram-negative bacteria.
753 *Microbiol Rev* **57**: 50-108.
754 Qiao, S., Q. Luo, Y. Zhao, X.C. Zhang and Y. Huang (2014) Structural basis for
755 lipopolysaccharide insertion in the bacterial outer membrane. *Nature* **511**: 108-111.
756 Ricci, D.P. and T.J. Silhavy (2012) The Bam machine: a molecular cooper. *Biochim Biophys Acta*
757 **1818**: 1067-1084.
758 Ruiz, N., S.S. Chng, A. Hiniker, D. Kahne and T.J. Silhavy (2010) Nonconsecutive disulfide
759 bond formation in an essential integral outer membrane protein. *Proc Natl Acad Sci U S*
760 *A* **107**: 12245-12250.
761 Ruiz, N., B. Falcone, D. Kahne and T.J. Silhavy (2005) Chemical conditionality: a genetic
762 strategy to probe organelle assembly. *Cell* **121**: 307-317.
763 Scheufler, C., A. Brinker, G. Bourenkov, S. Pegoraro, L. Moroder, H. Bartunik, *et al.* (2000)
764 Structure of TPR domain–peptide complexes. *Cell* **101**: 199-210.
765 Sheldrick, G.M. (2010) Experimental phasing with SHELXC/D/E: combining chain tracing with
766 density modification. *Acta Crystallogr D Biol Crystallogr* **66**: 479-485.
767 Shimoike, T., T. Taura, A. Kihara, T. Yoshihisa, Y. Akiyama, K. Cannon, *et al.* (1995) Product of
768 a new gene, *syd*, functionally interacts with SecY when overproduced in *Escherichia coli*.
769 *J Biol Chem* **270**: 5519-5526.
770 Shiota, T., K. Imai, J. Qiu, V.L. Hewitt, K. Tan, H.H. Shen, *et al.* (2015) Molecular architecture
771 of the active mitochondrial protein gate. *Science* **349**: 1544-1548.
772 Sikorski, R.S., M.S. Boguski, M. Goebl and P. Hieter (1990) A repeating amino acid motif in
773 CDC23 defines a family of proteins and a new relationship among genes required for
774 mitosis and RNA synthesis. *Cell* **60**: 307-317.
775 Sklar, J.G., T. Wu, L.S. Gronenberg, J.C. Malinverni, D. Kahne and T.J. Silhavy (2007)

For Peer Review

776 Lipoprotein SmpA is a component of the YaeT complex that assembles outer membrane
777 proteins in *Escherichia coli*. *Proc Natl Acad Sci U S A* **104**: 6400-6405.
778 Soltes, G.R., N.R. Martin, E. Park, H.A. Sutterlin and T.J. Silhavy (2017) Distinctive roles for
779 periplasmic proteases in the maintenance of essential outer membrane protein assembly.
780 *J Bacteriol*.
781 The UniProt Consortium (2017) UniProt: the universal protein knowledgebase. *Nucleic Acids*
782 *Res* **45**: D158-D169.
783 Tsukazaki, T., H. Mori, S. Fukai, T. Numata, A. Perederina, H. Adachi*, et al.* (2006) Purification,
784 crystallization and preliminary X-ray diffraction of SecDF, a translocon-associated
785 membrane protein, from *Thermus thermophilus*. *Acta Crystallogr Sect F Struct Biol*
786 *Cryst Commun* **62**: 376-380.
787 Warner, L.R., P.Z. Gatzeva-Topalova, P.A. Doerner, A. Pardi and M.C. Sousa (2017) Flexibility
788 in the periplasmic domain of BamA is important for function. *Structure* **25**: 94-106.
789 Wu, T., J. Malinverni, N. Ruiz, S. Kim, T.J. Silhavy and D. Kahne (2005) Identification of a
790 multicomponent complex required for outer membrane biogenesis in *Escherichia coli*.
791 *Cell* **121**: 235-245.
792 Wu, T., A.C. McCandlish, L.S. Gronenberg, S.S. Chng, T.J. Silhavy and D. Kahne (2006)
793 Identification of a protein complex that assembles lipopolysaccharide in the outer
794 membrane of *Escherichia coli*. *Proc Natl Acad Sci U S A* **103**: 11754-11759.
795 Zeytuni, N., D. Baran, G. Davidov and R. Zarivach (2012) Inter-phylum structural conservation
796 of the magnetosome-associated TPR-containing protein, MamA. *J Struct Biol* **180**:
797 479-487.
798 Zeytuni, N. and R. Zarivach (2012) Structural and functional discussion of the tetra-trico-peptide
799 repeat, a protein interaction module. *Structure* **20**: 397-405.

For Peer Review

800

801

For Peer Review

802 **Table 1. Data collection and refinement statistics for the BepA TPR domain**

	Se-Met-labeled $BepA_{310-482}$		
	peak	edge	remote
Data collection			
Space group	*R*32	*R*32	*R*32
Wavelength	0.9787	0.9794	0.9900
Resolution range (Å)	50 - 1.70 (1.76 - 1.70)	50 - 1.70 (1.73 - 1.70)	50 - 1.70 (1.73 - 1.70)
Unit cell			
a, b, c (Å)	104.0, 104.0, 81.5	104.2, 104.2, 81.7	104.2, 104.2, 81.7
α, β, γ (°)	90, 90, 120	90, 90, 120	90, 90, 120
Total reflections	1,833,668	947,226	941,228
Unique reflections	18,804 (1833)	18,967 (865)	18,975 (903)
Redundancy	38.1 (24.8)	17.7 (5.1)	18.9 (9.7)
Completeness (%)	99.8 (98.3)	99.7 (93.9)	99.9 (98.8)
Mean I/sigma(I)	24.7 (2.39)	20.1 (0.64)	25.5 (1.33)
R-merge	0.273 (0.992)	0.351 (1.40)	0.11 (1.083)
R-pim	0.047 (0.188)	0.088 (0.576)	0.025 (0.334)
CC1/2	0.999 (0.856)	0.998 (0.293)	1.00 (0.657)
Refinement			
Number of reflections	18,802 (1,833)		
R-work / R-free	16.8 / 19.9		
	(27.3 / 31.3)		
Number of non-hydrogen atoms	1,561		
macromolecules	1,376		
solvent	185		
Protein residues	175		
R.m.s. deviations			
Bonds (Å)	0.006		
Angles (°)	0.78		
Ramachandran			
favored (%)	98.27		
allowed (%)	1.73		
outliers (%)	0		
Average B-factor	22.8		
macromolecules	21.6		
solvent	31.4		

For Peer Review

803 **Table 2. Proteins identified by mass spectrometry analysis from the cross-linked adducts with BepA.**

Residue of BepA	XL-products* No.	Protein	Score	Peptide Matches
N323	1	LptD	113	2
		BamD	245	6
	2	LptD	68	1
		BamD	151	3
		YdgA	1,135	28
	3	BamD	172	3
		OmpA	364	9
	4	LptD	57	1
		BamD	2,167	55
		BamA	113	3
		OmpA	260	5
N364	1	BepA(dimer)	9,784	227
		OmpA	5,545	125
	2	OmpA	1,264	30
F404	1	BamA	8,550	197
		LptD	98	1
		BamD	446	10
		OmpA	176	4
	2	BamA	1,245	33
		LptD	74	1
		BamD	179	3
		OmpA	622	15
S455	1	BamC	101	2
		BamA	133	3
K458	1	LoiP	3,123	70
		BamC	959	17
		BamA	126	3
		OmpA	1,381	31
S461	1	BamA	1,172	30
		OmpA	384	11
	2	BamC	1,086	19
		OmpA	2,125	48
		BamA	334	9

804 *Numbers indicate the ones of the cross-linked (XL) products shown in s Supporting Information Fig. S5

Figure Legends

Figure 1. The TPR domain is required for BepA function.

A. Accumulation of C-terminally truncated forms of BepA. Δ*bepA* cells carrying pUC18 (vector), pUC-bepA, or a derivative of pUC-bepA having an amber mutation at the indicated positions were grown at 30°C in L medium supplemented with 1 mM IPTG. Total cellular proteins were analyzed by SDS-PAGE and immunoblotting. A schematic representation of BepA domain organization is shown above. SP, signal peptide. The result shown is a representative of two independent experiments that was conducted using the same transformant (i.e. two technical replicates).

B. Erythromycin sensitivity and accumulation of $LptD^{C}$ in Δ*bepA* or wild-type cells expressing the truncated forms of BepA. Total cellular proteins were analyzed by SDS-PAGE under reducing (+ME) or non-reducing (− ME) conditions and immunoblotting with anti-LptD (upper two panels) or anti-BepA (bottom panel) antibodies. $LptD^{NC}$, $LptD^{C}$, and $LptD^{RED}$ indicate LptD with non-consecutive disulfide bonds, LptD with consecutive disulfide bonds, and reduced LptD, respectively. BepA(FL) and BepA(Tr) indicate the full-length and truncated forms of BepA, respectively. The immunoblotting results shown are representatives of three technical replicates. The minimum inhibitory concentration (MIC) of erythromycin for each of the cells expressing BepA or its derivative were determined in the presence of 1 mM IPTG at 30°C as described in Materials and methods. The MIC assay result shown is a representative of two biological replicates. The MIC data of these replicates are shown in Supporting Information Fig. S1A, which shows that, although there are some fluctuations, difference in the MIC values are essentially reproducible and thus

For Peer Review

829 significant. Δ*bepA* cells carrying plasmid encoding the protease active site mutant
830 (E137Q) of BepA exhibited increased sensitivity to erythromycin as compared with
831 those carrying an empty plasmid (vector). This could be due to some deleterious effects
832 of the BepA(E137Q) protein on cell viability.
833
834 Figure 2. Crystal Structure of the BepA TPR domain.
835 A. Amino acid sequence of the BepA TPR domain. The TPR modules and non-TPR
836 helices (nTH) are indicated. The loop regions between the individual TPR modules are
837 designated as L1 to L5, and the region C-terminal to nTH2 is designated as C.
838 B. Crystal structure of BepA TPR domain (ribbon model). α-helices are colored as in *A*.
839 The large palm with a pocket and the small palms with a cavity are indicated. Acidic
840 residues in the pocket are highlighted in ball-and-stick form.
841 C. Surface representations colored according to electrostatic potential ranging from blue
842 (+10 kT/e) to red (−10 kT/e).
843
844 Figure 3. pBPA-mediated cross-linking of the BepA TPR domain.
845 Δ*bepA* cells carrying pEVOL-pBpF and pUC-bepA-his$_{10}$ (WT) encoding BepA$_{His10}$ or its
846 derivative with an amber mutation at the indicated position were grown in L medium
847 supplemented with 1 mM pBPA, 1 mM IPTG, and 0.2% arabinose, before being
848 UV-irradiated for 0 (−) or 10 min (+). Total cellular proteins were analyzed by
849 SDS-PAGE and immunoblotting with anti-BepA antibody. The results shown are
850 representatives of two technical replicates. Bars over amino acid residue numbers are
851 colored according to those in Fig. 2A.
852

For Peer Review

Figure 4. Cross-linking of BepA with the BAM complex components.

A-C. Cross-linking of BepA with BamA, BamC, and BamD. Δ*bepA* cells carrying pEVOL-pBpF and a derivative of either pUC-bepA-his_{10} (A and B) or pUC-bepA (C) with an amber codon and the E137Q mutation (A and C) or with only an amber mutation (B) were grown in L medium and UV-irradiated as described in the legend to Fig. 3. For A and B, membrane fractions were prepared by sonic disruption of cells followed by ultracentrifugation. Proteins from the membrane fractions (A and B) and from whole cells (C) were analyzed by SDS-PAGE and immunoblotting with antibodies against BepA (lower panels) or respective BAM components (upper panels). The cross-linked products of BepA with BamA, BamC, and BamD are indicated by BepA×BamA, BepA×BamC and BepA×BamD, respectively. Asterisks indicate cross-linked adducts with unidentified proteins. The results shown in A-C are representatives of two technical replicates.

D. Mapping of sites of cross-linking with BamA (green), BamC (red), and BamD (yellow) onto the structure of the BepA TPR domain (see text and Fig. 2). The same view as Fig. 2B is shown.

Figure 5. Cross-linking of BamA with BepA.

A. Cross-linking of BamA(pBPA) with BepA. Cells of a BamA depletion strain carrying pSup-BpaRS-6TRN and a plasmid encoding a $_{His6}$BamA derivative with an amber mutation at the indicated position were grown at 37°C in L medium supplemented with 0.2% glucose and 1 mM pBPA. His6-tagged proteins were affinity-purified and analyzed by SDS-PAGE and immunoblotting with antibodies against BepA (lower panel) or BamA (upper panel). The cross-linked products between BamA and BepA are indicated

For Peer Review

877 by BamA×BepA. An asterisk indicates a cross-linked adduct with an unidentified protein.
878 The result is a representative of two independent experiments that were conducted using
879 two independently isolated transformants (i.e. two biological replicates).
880 B. Location of E224 (orange sphere) in BamA of a BAM complex structure (PDB code:
881 5D0O). BamA is shown in green, BamB in cyan, BamC in red, BamD in yellow, and
882 BamE in gray.
883
884 Figure 6. pBPA-mediated cross-linking between the BepA TPR domain and LptD.
885 A and B. Cross-linking of BepA(N323pBPA) and BepA(F404pBPA) with LptD. Δ*bepA*
886 cells carrying pEVOL-pBpF and pUC-bepA-his$_{10}$ derivatives encoding
887 BepA(N323amber)$_{His10}$, BepA(N323amber/E137Q)$_{His10}$, BepA(F404amber)$_{His10}$, or
888 BepA(F404amber/E137Q)$_{His10}$ were grown and UV-irradiated for 10 min as described in
889 the legend to Fig. 3. After sonic disruption of cells, the His10-tagged proteins and their
890 cross-linked adducts were affinity-purified and analyzed by SDS-PAGE and
891 immunoblotting. Proteins from approximately four-fold more cells were loaded on the
892 gel for the BepA(N323pBPA) and BepA(F404pBPA) samples compared to the
893 BepA(N323pBPA/E137Q) and BepA(F404pBPA/E137Q) samples, because lower
894 amounts of the His-tagged proteins were recovered for the WT samples, due to
895 self-cleavage of the C-terminally attached His tag (see Fig. 8C and D). The bands
896 indicated by asterisks were apparently reacted with both anti-BepA and anti-LptD
897 antibodies and thus might contain degradation products of the BepA-LptD cross-linked
898 adducts.
899 C. Growth phase-dependent cross-linking of BepA with LptD. Δ*bepA* cells carrying
900 pEVOL-pBpF and pUC-bepA(N323amber/E137Q)-his$_{10}$ were grown in M9 medium

For Peer Review

supplemented with 1 mM pBPA, 1 mM IPTG, and 0.2% arabinose at 30°C and a portion was withdrawn at the indicated time points (left). Following UV-irradiation for 10 min, total cellular proteins were analyzed by SDS-PAGE and immunoblotting (right). The results shown in A-C are representatives of three (for A and C) or two (for B) technical replicates.

D. Mapping of sites of cross-linking with LptD (purple) onto the structure of the BepA TPR domain (see text and Fig. 2). The same view as Fig. 2B left and Fig. 4D left is shown.

Figure 7. Effects of F404 mutations on the function and the protein-protein interaction.

A and B. Erythromycin sensitivity (upper panels) and accumulation of $LptD^{C}$ and BepA (middle and lower panels, respectively) in Δ*bepA* cells expressing BepA mutants. Wild-type cells (chrom) or Δ*bepA* cells carrying pUC18 (vector), pUC-bepA (WT), pUC-bepA(E137Q) (E137Q), or a derivative of pUC-bepA encoding a BepA mutant having Ala at the LptD-cross-linking site (N323), BamD-cross-linking site (D444), or BamA-cross-linking site (N397, F404, Q428, or R480) (A), or having an amino acid alteration to various residues at F404 (B) were used. The MICs of erythromycin for the above cells were determined at 30°C in the absence of IPTG. For immunoblotting analysis, cells were grown in L medium at 30°C and total cellular proteins were subjected to SDS-PAGE under non-reducing conditions and probed with anti-LptD or anti-BepA antibodies.

C. Effect of F404 mutations on the cross-linking of BepA with BamA, BamC, BamD, or LptD. Δ*bepA* cells carrying pEVOL-pBpF and a plasmid encoding a BepA derivative having the Q428amber, L459amber, or D444amber mutation, or the E137Q/N323amber

For Peer Review

925 mutations, with or without the F404G or F404Y mutation, were grown in L medium
926 supplemented with 1 mM pBPA, 1 mM IPTG, and 0.2% arabinose, and UV-irradiated for
927 10 min. The membrane fractions were acid-precipitated and analyzed by SDS-PAGE and
928 immunoblotting with anti-BepA antibody. Asterisks indicate cross-linked adducts with
929 unidentified proteins. The entire blots for the data in C are shown in Fig. S6 to show
930 loading controls. The MIC assay results shown in A and B are representatives of three
931 biological replicates. The MIC data of these replicates are shown in Supporting
932 Information Fig. S1B, which shows that, although there are some fluctuations, difference
933 in the MIC values are essentially reproducible and thus significant. The immunoblotting
934 results are representatives of two technical replicates.
935
936 Figure 8. Effects of the F404 mutations on the substrate degradation and self-cleavage.
937 A. degradation of overexpressed LptD by BepA F404 mutants. Δ*bepA* cells carrying
938 pTWV-lptD-his$_{10}$ and either pSTD689 (vector) or pSTD-bepA derivatives were grown at
939 30°C in L medium without IPTG. Total cellular proteins were analyzed by SDS-PAGE
940 and immunoblotting with anti-LptD (upper panel), anti-penta-His (middle panel), and
941 anti-BepA (lower panel) antibodies. In the upper panel, bands indicated by LptD
942 contained both chromosomally and ectopically expressed LptD. Arrowheads indicate
943 degradation products of LptD.
944 B. degradation of BamA by BepA F404 mutants in the Δ*surA* strain. Δ*surA* Δ*bepA*
945 double mutant cells carrying pUC18 (vector) or a pUC-bepA derivative were grown at
946 30°C in M9 medium supplemented with 1 mM IPTG. Total cellular proteins were
947 analyzed by SDS-PAGE and immunoblotting with anti-BamA (upper panel) and
948 anti-BepA (lower panel) antibodies. The arrowhead indicates a BamA degradation

For Peer Review

949 product.

950 C. Intramolecular self-cleavage of BepA. Δ*bepA* cells carrying pUC18 (vector),
951 pUC-bepA (WT) or pUC-bepA(E137Q) (E137Q) were further transformed with
952 pTH-bepA-his$_{10}$ (WT-His) or pTH-bepA(E137Q)-his$_{10}$ (E137Q-His). Cells were grown
953 at 30°C in L medium without IPTG. Total cellular proteins were analyzed by SDS-PAGE
954 and immunoblotting with anti-BepA antibody. "Cleaved" indicates self-cleaved
955 BepA$_{His10}$.

956 D. Effects of the F404 mutations on BepA self-cleavage. Δ*bepA* cells carrying a
957 pTH-bepA derivative encoding the indicated F404 mutant form of BepA$_{His10}$ were grown
958 at 30°C in L medium without IPTG. Total cellular proteins were analyzed by SDS-PAGE
959 and immunoblotting with anti-BepA antibody. An asterisk indicates a non-specific band
960 serving as a loading control. The results are representatives of two biological replicates.

961

962 Figure 9. A conceptual docking model between the BAM complex and BepA.

963 A-C. The crystal structure of the BepA TPR domain was manually associated with a
964 crystal structure of the BAM complex (PDB code: 5D0O). Lateral (A) and periplasmic
965 side (B and C) views are shown. BamA, B, C, D, E, and BepA are shown by ribbons in
966 green, cyan, red, yellow, gray, and orange, respectively. The BepA residues cross-linked
967 with the BAM components and a BamA residue cross-linked with BepA are indicated by
968 spheres with the same color as the corresponding BAM components and BepA,
969 respectively.

970

971 Figure 10. Two models for BepA function in the assembly of LptD.

972 A. First model. BepA interacts with LptD in the periplasmic space (i) and the complex is

For Peer Review

973 then targeted to the BAM complex for assembly of LptD into the outer membrane (ii).
974 B. Second model. BepA is first associated with the BAM complex (i) and accepts LptD
975 on the BAM complex to promote its assembly (ii). In either case, it would be possible
976 that the first interaction facilitates the following interaction, that is, in the first model,
977 productive interaction between BepA and LptD might promote the following interaction
978 of BepA (or BepA-LptD) with the BAM complex, whereas in the second model, prior
979 interaction of BepA with the BAM complex might facilitate the following interaction of
980 BepA (or BepA-BAM) with LptD. Note that regardless of the step at which BepA
981 functions, the interaction of BepA with the BAM complex and with LptD is not essential
982 for LptD assembly, since LptD can assemble into the functional LptD/LptE complex
983 even in the absence of BepA, although LptD assembly is significantly retarded when the
984 BepA function is impaired. Thus, BepA is required for efficient assembly of LptD. BepA
985 is also involved in degradation of OMPs including LptD when their normal assembly is
986 compromised.

For Peer Review

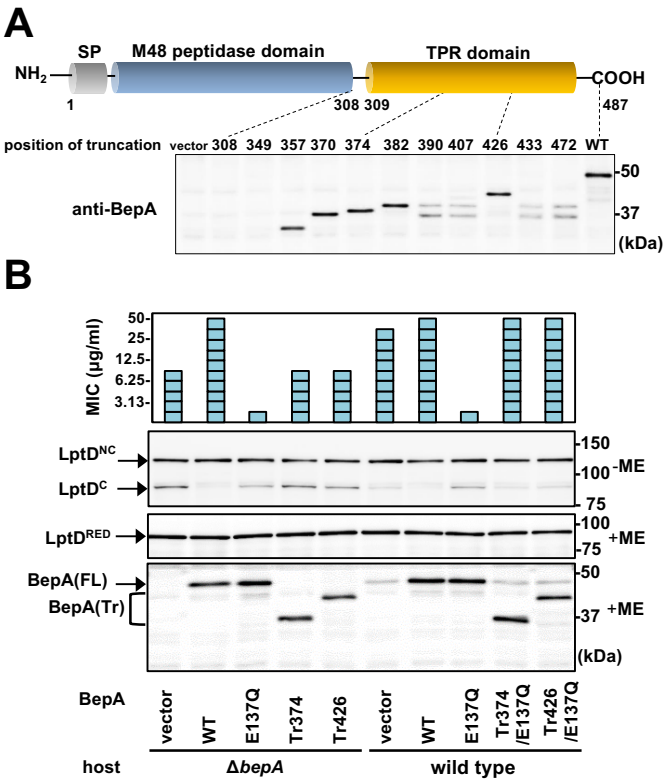
A
SP
M48 peptidase domain
TPR domain
NH2
COOH
1
308 309
487
position of truncation vector 308 349 357 370 374 382 390 407 426 433 472 WT
anti-BepA
50
37
(kDa)
B
MIC (μg/ml)
50
25
12.5
6.25
3.13
LptDNC
LptDC
LptDRED
150
100
75
-ME
+ME
BepA(FL)
BepA(Tr)
50
37
BepA
vector
WT
E137Q
Tr374
Tr426
vector
WT
E137Q
Tr374 /E137Q
Tr426 /E137Q
host
ΔbepA
wild type

Figure 1

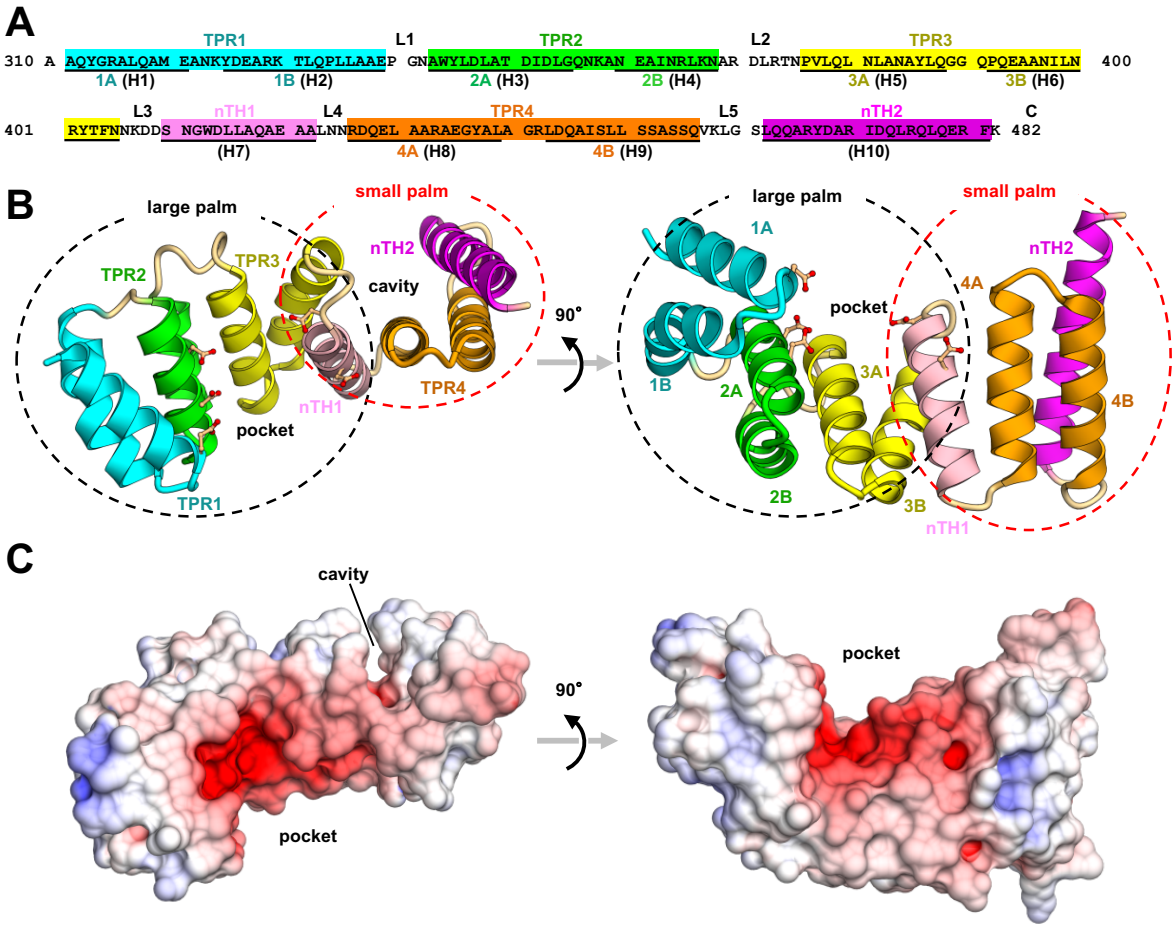
A
TPR1
L1
TPR2
L2
TPR3
310 A AQYGRALQAM EANKYDEARK TLQPLLAAEP GNAWYLDLAT DIDLGQNKAN EAINRLKNAR DLRTNPVLQL NLANAYLQGG QPQEAANILN 400
1A (H1)
1B (H2)
2A (H3)
2B (H4)
3A (H5)
3B (H6)
L3
nTH1
L4
TPR4
L5
nTH2
C
401 RYTFNNKDDS NGWDLLAQAE AALNNRDQEL AARAEGYALA GRLDQAISLL SSASSQVKLG SLQQARYDAR IDQLRQLQER FK 482
(H7)
4A (H8)
4B (H9)
(H10)
B
large palm
small palm
TPR2
TPR3
nTH2
cavity
TPR4
nTH1
pocket
TPR1
90°
large palm
small palm
1A
nTH2
pocket
4A
1B
2A
3A
4B
2B
3B
nTH1
C
cavity
pocket
90°
pocket

Figure 2

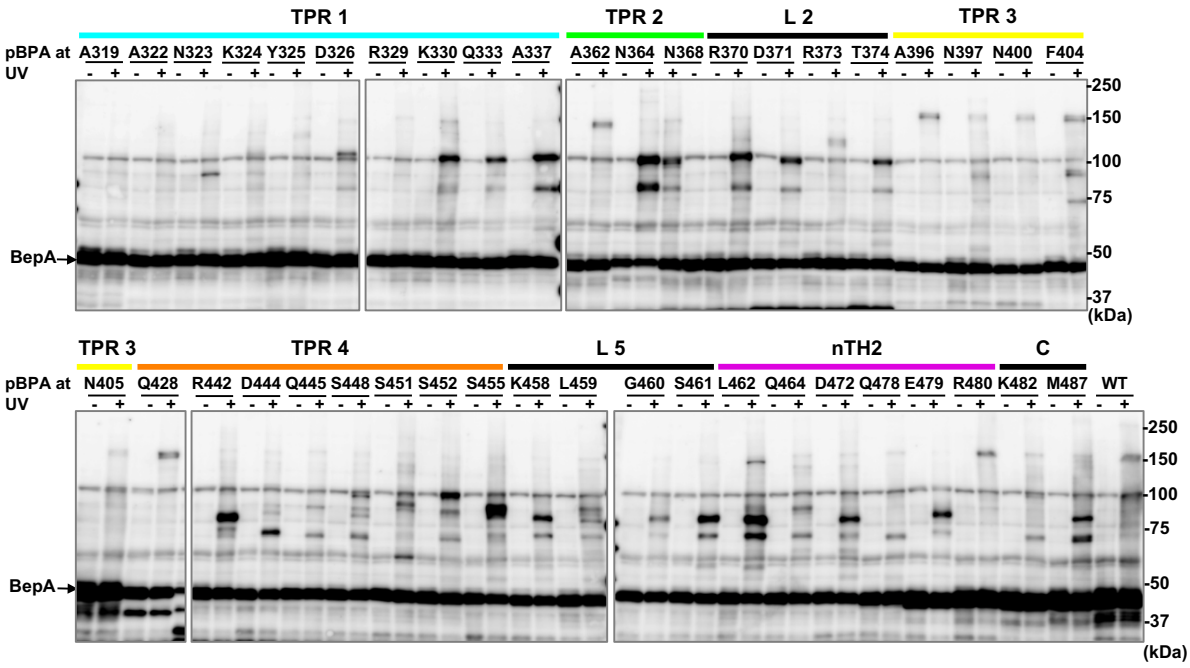
TPR 1
TPR 2
L 2
TPR 3
pBPA at A319 A322 N323 K324 Y325 D326 R329 K330 Q333 A337 A362 N364 N368 R370 D371 R373 T374 A396 N397 N400 F404
UV
BepA
250
150
100
75
50
37
(kDa)
TPR 3
TPR 4
L 5
nTH2
C
pBPA at N405 Q428 R442 D444 Q445 S448 S451 S452 S455 K458 L459 G460 S461 L462 Q464 D472 Q478 E479 R480 K482 M487 WT
UV
BepA
250
150
100
75
50
37
(kDa)

Figure 3

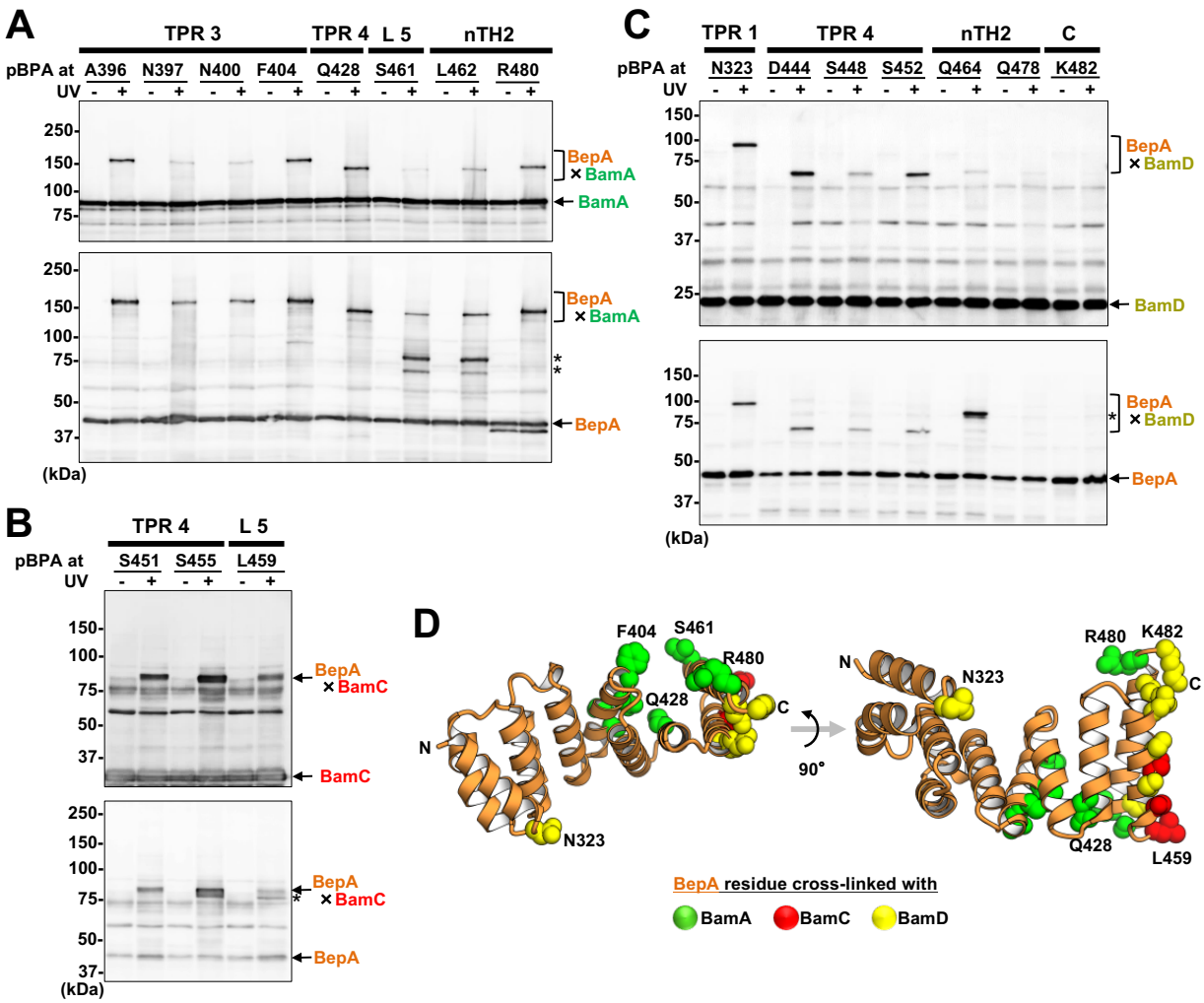
A
TPR 3
TPR 4
L 5
nTH2
pBPA at
A396
N397
N400
F404
Q428
S461
L462
R480
UV
BepA
× BamA
BamA
BepA
× BamA
BepA
(kDa)
B
TPR 4
L 5
pBPA at
S451
S455
L459
BepA
× BamC
BamC
BepA
× BamC
BepA
(kDa)
C
TPR 1
TPR 4
nTH2
C
pBPA at
N323
D444
S448
S452
Q464
Q478
K482
BepA
× BamD
BamD
BepA
× BamD
BepA
(kDa)
D
F404
S461
R480
Q428
N
C
N323
90°
N
N323
R480
K482
C
Q428
L459
BepA residue cross-linked with
BamA
BamC
BamD

Figure 4

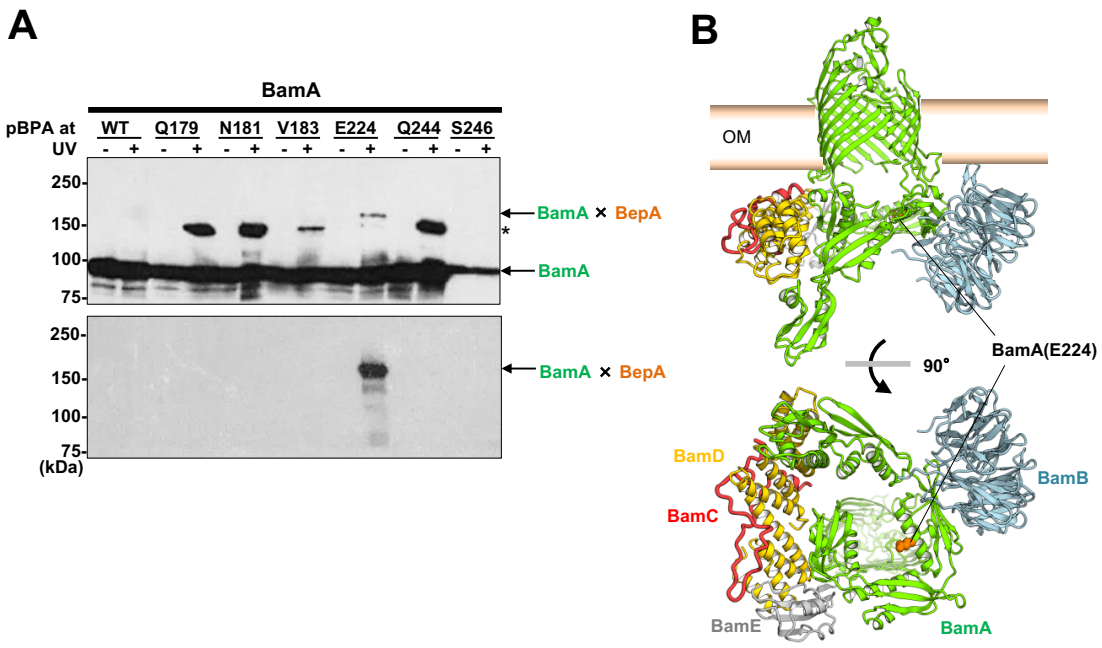
A
BamA
pBPA at
UV
WT
Q179
N181
V183
E224
Q244
S246
250
150
100
75
(kDa)
BamA × BepA
*
BamA
BamA × BepA
B
OM
90°
BamA(E224)
BamD
BamC
BamB
BamE
BamA

Figure 5

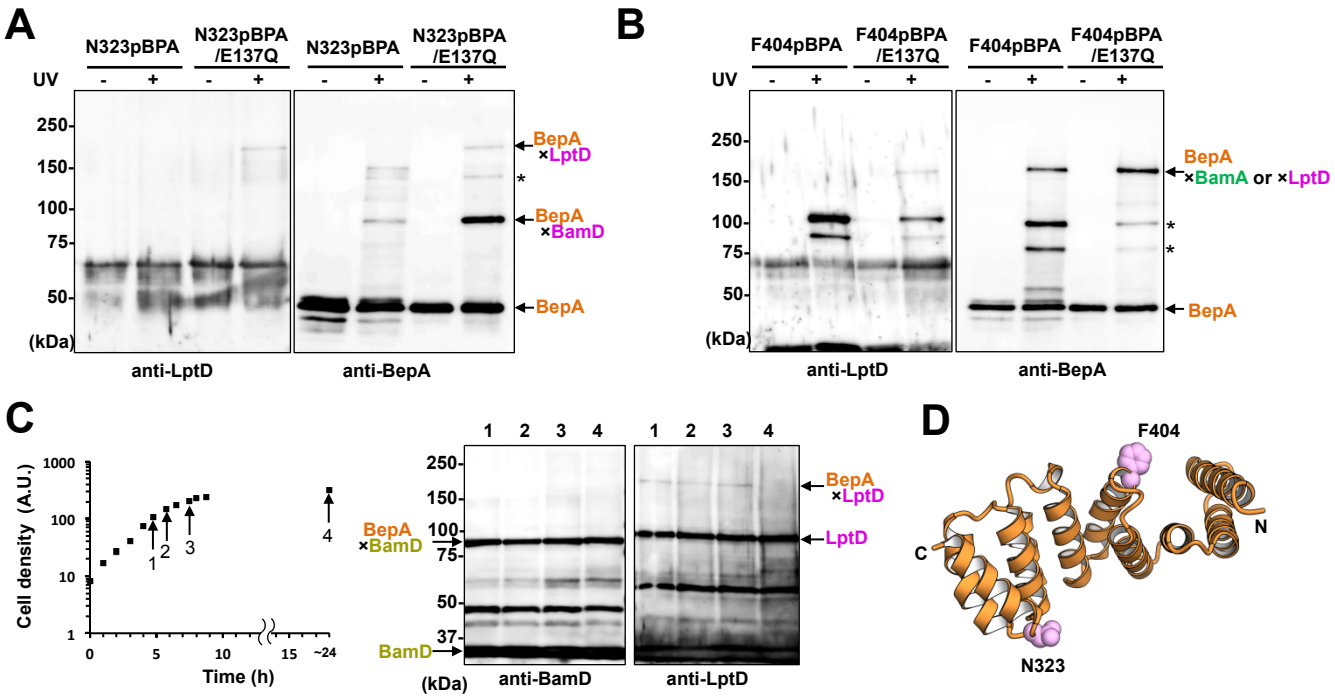
A
N323pBPA
N323pBPA /E137Q
N323pBPA
N323pBPA /E137Q
UV
- + - + - + - +
250
150
100
75
50
(kDa)
BepA ×LptD
*
BepA ×BamD
BepA
anti-LptD
anti-BepA
B
F404pBPA
F404pBPA /E137Q
F404pBPA
F404pBPA /E137Q
UV
- + - + - + - +
250
150
100
75
50
(kDa)
BepA ×BamA or ×LptD
*
*
BepA
anti-LptD
anti-BepA
C
Cell density (A.U.)
1000
100
10
1
0
5
10
15
~24
Time (h)
1
2
3
4
1 2 3 4 1 2 3 4
250
150
100
75
50
37
(kDa)
BepA ×BamD
BamD
BepA ×LptD
LptD
anti-BamD
anti-LptD
D
F404
C
N
N323

Figure 6

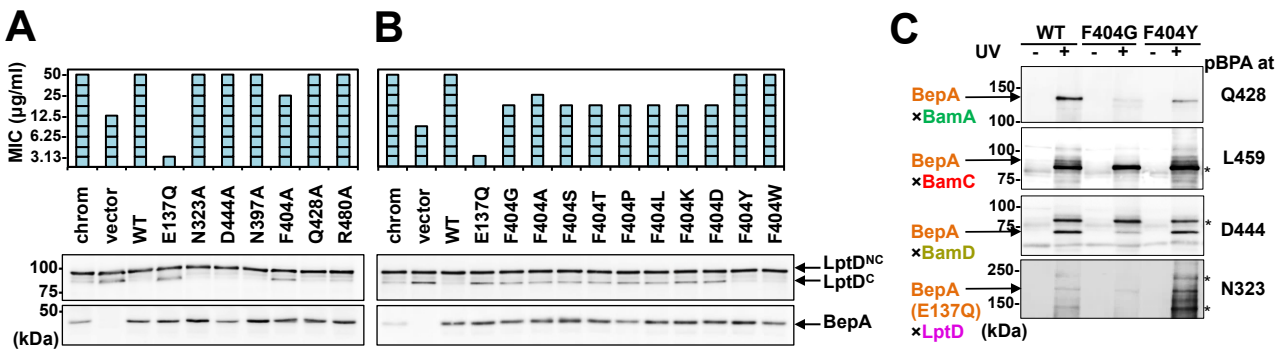
A
B
C
MIC (μg/ml)
50
25
12.5
6.25
3.13
chrom
vector
WT
E137Q
N323A
D444A
N397A
F404A
Q428A
R480A
F404G
F404S
F404T
F404P
F404L
F404K
F404D
F404Y
F404W
100
75
50
(kDa)
LptDNC
LptDC
BepA
UV
WT
F404G
F404Y
pBPA at
BepA
×BamA
×BamC
×BamD
×LptD
150
100
75
250
Q428
L459
D444
N323
(E137Q)

Figure 7

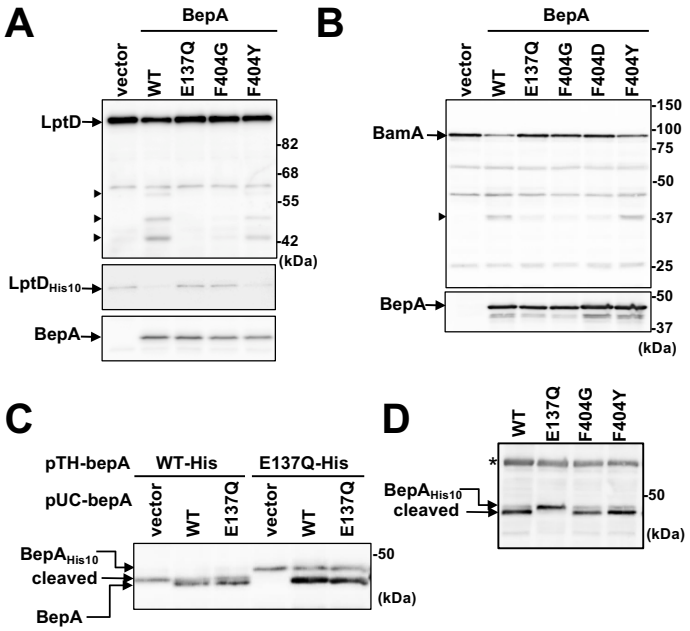
A
BepA
vector
WT
E137Q
F404G
F404Y
LptD
82
68
55
42
(kDa)
LptD$_{His10}$
BepA
B
BepA
vector
WT
E137Q
F404G
F404D
F404Y
BamA
150
100
75
50
37
25
BepA
50
37
(kDa)
C
pTH-bepA
WT-His
E137Q-His
pUC-bepA
vector
WT
E137Q
vector
WT
E137Q
BepA$_{His10}$
cleaved
BepA
50
(kDa)
D
WT
E137Q
F404G
F404Y
*
BepA$_{His10}$
cleaved
50
(kDa)

Figure 8

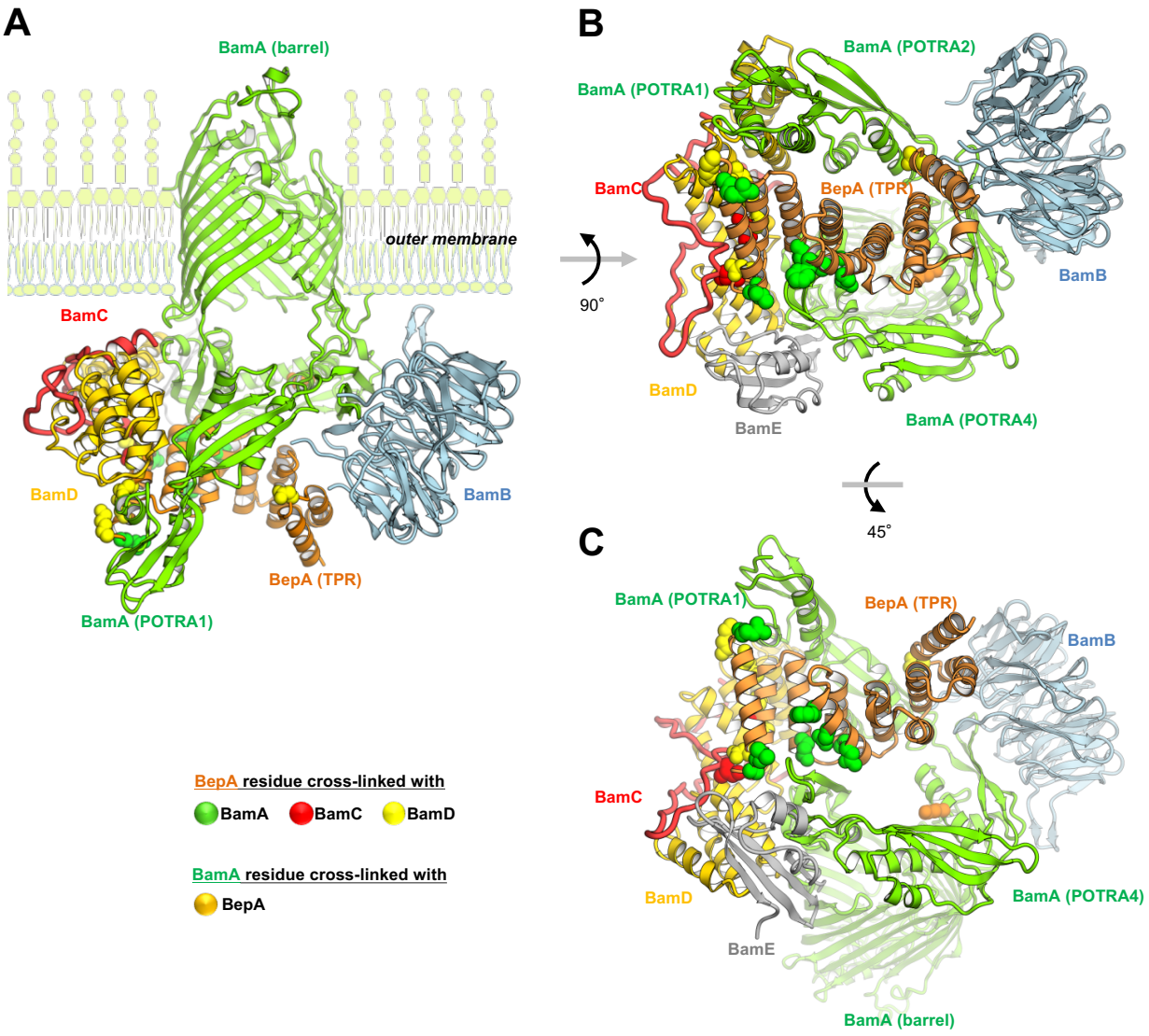
A
BamA (barrel)
outer membrane
BamC
BamD
BamB
BepA (TPR)
BamA (POTRA1)
BepA residue cross-linked with
BamA
BamC
BamD
BamA residue cross-linked with
BepA
B
BamA (POTRA2)
BamA (POTRA1)
BamC
BepA (TPR)
BamB
90˚
BamD
BamE
BamA (POTRA4)
45˚
C
BamA (POTRA1)
BepA (TPR)
BamB
BamC
BamD
BamA (POTRA4)
BamE
BamA (barrel)

Figure 9

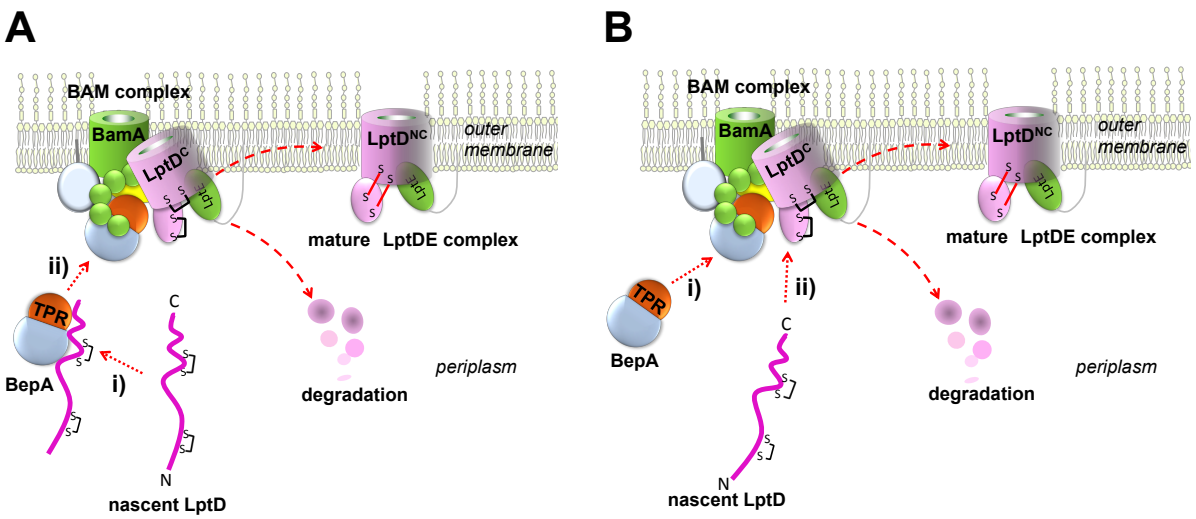
A
BAM complex
BamA
LptDC
LptDNC
outer membrane
mature LptDE complex
ii)
TPR
BepA
i)
C
N
nascent LptD
degradation
periplasm
B
BAM complex
BamA
LptDC
LptDNC
outer membrane
mature LptDE complex
TPR
BepA
i)
ii)
C
N
nascent LptD
degradation
periplasm

Figure 10